



universität
wien

MASTERARBEIT

Titel der Masterarbeit

„Inhibition of fatty acid synthase (FASN) in ovarian cancer cells: Evaluation of a novel therapeutic strategy based on proteomics and metabolomics profiling“

verfasst von

Mariya Semkova (BSc)

angestrebter akademischer Grad

Master of Science (MSc)

Wien, 2015

Studienkennzahl lt. Studienblatt: A 066 862

Studienrichtung lt. Studienblatt: Masterstudium Chemie

Betreut von: Univ.-Prof. Dr. Christopher Gerner

Abstract

Fatty acid synthase (FASN) is an important metabolic enzyme which, under certain conditions, has oncogenic potential and is able to play an important role in tumor growth and survival. Development of appropriate anticancer agents targeting the FASN activity is still under progress. Here we demonstrate the cytostatic and cytotoxic effects induced by the FASN inhibitor UCMG028 in the ovarian cancer cell line SKOV3. This was achieved by isolation of protein and metabolite fractions from treated and untreated cells after 8h and 24h of incubation. Proteome changes were detected via MS based shotgun proteome profiling with subsequent data evaluation using MaxQuant, while changes of selected metabolites were investigated using an MRM based metabolomics assay. The obtained data show impaired phospholipid biosynthesis, leading to cell cycle and cell growth arrest. This was accompanied by induction of programmed cell death via the mitochondrial pathway. Several oncogenic signaling pathways such as MAPK, NFκB and Ras also showed down-regulation. As a conclusion, UCMG028 seems to be a promising agent for therapy of ovarian malignancies.

Zusammenfassung

Die Fettsäure-Synthase (FASN) ist ein wichtiges metabolisches Enzym, das unter bestimmten Bedingungen, ein onkogenes Potential aufweisen kann und in der Lage ist, das Wachstum und das Überleben von Krebszellen zu stimulieren. Somit ist die Fettsäure-Synthase ein attraktives Target für die Therapie von einigen Tumorarten, unter anderem auch von Ovarialkarzinomen, was zur Entwicklung von Fettsäure-Synthase inhibierenden Medikamenten geführt hat. UCMG028 ist ein solcher Inhibitor. Im Rahmen dieser Masterarbeit wurde gezeigt, dass der Fettsäure-Synthase Inhibitor UCMG028 tatsächlich zytostatische und zytotoxische Effekte auf SKOV3 Ovarialkarzinomzellen hat. Dafür wurden Protein- und Metabolitenfraktionen, isoliert aus behandelten und nicht behandelten Zellen nach 8- bzw. 24-stündiger Inkubation mit dem Inhibitor, untersucht. Änderungen im Proteom wurden mittels MS basierendem Shotgun Proteom Profiling mit nachfolgender MaxQuant Analyse nachgewiesen, während quantitative Änderungen von bestimmten Metaboliten durch eine targeted Metabolomics Analyse mit Hilfe von multiple reaction monitoring (MRM) bestimmt wurden. Die Ergebnisse zeigen eine Störung der Phospholipidbiosynthese, die zu einer Hemmung des Zellzyklus und des Zellwachstums führt. Des Weiteren wurde die Induzierung von Apoptose über den mitochondrialen Signalweg, sowie eine Runterregulierung der onkogenen MAPK, NFkB und Ras Signalwege beobachtet. Somit konnte gezeigt werden, dass sich UCMG028 sehr wohl als Kandidat für die Therapie von ovarialen Tumorerkrankungen eignen könnte.

Acknowledgments

I would like to thank Univ.-Prof. Dr. Christopher Gerner and Univ.-Prof. Mag. Dr. Thomas Grunt for the opportunity to participate on this interesting study.

I would also like to express my gratitude to Dr. Astrid Slany for her supervision and her help during the course of this project.

Finally I would like to thank the rest of the group for being very helpful. Special thanks are due to Dr. Samuel Meier for the measurements on the triple quadrupole mass spectrometer and for his expertise in metabolomics, Rupert Mayer, MSc, for his help during the preparation steps for the metabolomic assays, and Andrea Bileck, MSc, for her help during the cell culture experiment and the measurements on the orbitrap mass spectrometer.

Table of contents

1	Introduction.....	9
1.1	Introduction and aim.....	9
1.2	Fatty acid synthesis.....	10
1.3	Fatty acid synthase.....	13
1.3.1	Structure and biological function.....	13
1.3.2	Upregulation of FASN in cancer cells.....	14
1.3.3	FASN as a potential therapeutic target for cancer therapy.....	16
1.3.4	FASN inhibitors.....	20
1.4	Proteome profiling.....	21
1.4.1	Definition and goals of proteome profiling.....	21
1.4.2	Methods and tools of proteomics.....	22
1.4.2.1	Mass spectrometry based shotgun proteomics.....	22
1.4.2.2	Q Exactive Orbitrap Mass Spectrometer.....	24
1.4.2.3	Max Quant.....	26
1.5	Metabolomics.....	26
1.5.1	Definition and goals of metabolomics.....	26
1.5.2	Targeted metabolomics using multiple reaction monitoring (MRM).....	27
2	Methods.....	29
2.1	Cell culture experiments.....	29
2.1.1	Preparation of the cell culture medium.....	29
2.1.2	Cell culture and characterization of SKOV3 cells.....	29
2.1.3	Cell culture preparation for FASN inhibitor experiments.....	30
2.1.4	Incubation with UCMG028.....	30
2.2	Harvesting of cells.....	30
2.2.1	Harvesting of cells and preparation of protein extracts from cell cytoplasm and nuclei for proteomics experiments.....	30
2.2.2	Harvesting of cells and preparation of metabolite extracts from whole cell lysates for metabolomics experiments.....	31
2.2.3	Bradford assay.....	32
2.3	Shotgun proteomics.....	33
2.3.1	In-gel digestion.....	33
2.3.1.1	Preparation of 1D-SDS-acrylamide gel.....	33
2.3.1.2	Sample loading.....	34
2.3.1.3	SDS-gel electrophoresis.....	35
2.3.1.4	Silver staining.....	35
2.3.1.5	In-gel digestion.....	35
2.3.2	In-solution digestion.....	37
2.3.3	Mass spectrometry measurement.....	39
2.3.4	Data analysis.....	39
2.3.4.1	Proteome discoverer.....	39

2.3.4.2	Max Quant search.....	39
2.3.4.3	Max Quant data processing.....	41
2.4	Targeted metabolomics.....	41
2.4.1	Preparation of reagents and solvents.....	41
2.4.2	Preparation of Biocrates p180 Kit plate.....	43
2.4.3	Biocrates p180 Kit measurement.....	43
2.4.4	Data analysis.....	44
3	Results.....	45
3.1	Cell culture experiment.....	45
3.2	Proteome profiling.....	46
3.2.1	SKOV3 cell characterization.....	46
3.2.2	Proteome profiling after FASN inhibition.....	47
3.2.2.1	Down-regulated proteins.....	47
3.2.2.2	Upregulated proteins.....	58
3.3	Targeted metabolomics.....	62
3.3.1	Amino acids.....	62
3.3.2	Biogenic amines.....	64
3.3.3	Phospholipids.....	64
3.3.4	Acylcarnitines.....	67
3.3.5	Hexose.....	69
4	Discussion.....	70
5	Conclusion.....	73
	References.....	74
	Appendix.....	78
	Curriculum Vitae.....	86

List of abbreviations

ABC	Ammonium bicarbonate
ACN	Acetonitrile
ACP	Accessory gland protein
AKT	Serine/threonine kinase
APAF1	Apoptotic protease-activating factor 1
APD	Actin patches distal protein
Arf	ADP Ribosylation Factor
ATP	Adenosine triphosphate
BLAST	Basic local alignment search tool
CID	Collision induced dissociation
CoA	Coenzyme A
DTT	Dithiothreitol
4EBP1	Eukaryotic translation initiation factor 4E-binding protein 1
EGFR	Epidermal growth factor receptor
EMT	Epithelial-mesenchymal transition
EOC	Epithelial ovarian cancer
ER	Endoplasmic reticulum
ErbB1(2)	Receptor tyrosine-protein kinase erbB-1(2)
FA	Formic acid
FASN	Fatty acid synthase
FBI-1	Zinc finger and BTB domain-containing protein 7A
FBS	Fetal bovine serum
FIA	Flow injection analysis
FT	Fourier transformation
GHCl	Guanidinium hydrochloride
HCD	High energy collision dissociation
HPLC	High performance liquid chromatography
IAA	Iodoacetamide
IF4E	Eukaryotic translation initiation factor 4E
INK4A	Cyclin-dependent kinase inhibitor 2A
ISTD	Internal standard
LC	Liquid chromatography
MRM	Multiple reaction monitoring
MS	Mass spectrometry
m/z	Mass-to-charge ratio
NAD	Nicotinamide adenine dinucleotide
NADP ⁺	Nicotinamide adenine dinucleotide phosphate
NADPH	Nicotinamide adenine dinucleotide phosphate
NEDD4	E3 ubiquitin-protein ligase NEDD4
P _i	Phosphate
PEA3	ETS translocation variant 4
PIC	Protease inhibitor cocktail
PI3K	Phosphoinositide 3-kinase
PMSF	Phenylmethanesulfonylfluoride
pRb	Retinoblastoma protein

PTIC	Phenyl isothiocyanate
ROS	Reactive oxygen species
RP	Reversed phase
RP-HPLC	Reversed phase high performance liquid chromatography
SB	Sample buffer
SDS	Sodium dodecyl sulfate
SREBP-1c	Sterol regulatory element binding protein 1c
TFA	Trifluoroacetic acid
USP2a	Ubiquitin specific protease 2a
VDAC	Voltage-dependant anion channel

1. Introduction

1.1 Introduction and aim

For the last 30 years, anticancer research has been orientated towards the discovery of genetic alterations in oncogenic and tumor suppressor genes, as regulators of cell growth, migration and apoptosis. As a result, several drug targets have been identified and their corresponding therapeutics have been developed and added to the armamentarium in the fight against cancer. [1] However, in case of ovarian cancer, this approach has shown only limited benefits, [1] as this illness is still the most common cause of gynecologic cancer-related death worldwide. [2] Thus, especially for advanced ovarian cancer, novel therapeutic strategies are urgently needed. [1] For several years it has been known that cancer cells show alterations in their metabolic phenotype allowing them to adapt and survive dynamic microenvironmental conditions. [3] For instance, an enhanced glucose uptake known as the Warburg effect, accompanied by elevated lactate production and secretion by cancer cells suggests that aerobic glycolysis is their primary source of ATP synthesis. [3] Consequently, cancer cells are supplied with elevated amounts of bioenergy and building blocks for macromolecules (proteins, nucleic acids), essential for cell division. In addition, it was recently found that metabolic pathways closely interact with oncogenic networks, and that altered oncogenes and tumor suppressor genes directly affect cancer cell metabolism. [1]

A remarkable metabolic alteration in ovarian cancer cells is the hyperactivation of *de novo* synthesis of phospholipids, essential for membrane formation. Actually, the fatty acid synthase (FASN), which catalyzes the formation of palmitic acid - the precursor of all lipids - is overexpressed, which correlates with chemoresistance and tumor progression. Importantly, elevated expression of several proteins involved in cell growth signaling such as the epidermal growth factor receptor (EGFR), the receptor tyrosine-protein kinase (ErbB2) and the serine/threonine kinase (AKT) have been shown to correlate with FASN overexpression, which supports the theory of an existing link between oncogene pathways and metabolic systems. Inhibition of the FASN activity induces cell growth arrest and apoptosis, which suggests that targeting FASN could be a novel antimetabolic approach for ovarian cancer treatment. [1]

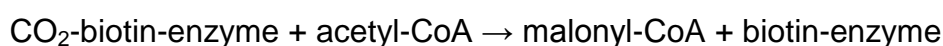
Several compounds are known to block FASN activity; however, none of them is suitable for clinical application due to their lack of potency and/or their severe side effects. [4] Therefore development of FASN targeting anticancer drugs is still under process. Recently, novel FASN blockers have been designed to overcome these limitations and are now subjected to clinical evaluation. It is hoped that at least a part of these promising agents will be able to exploit the full potential of FASN as a target for anticancer therapy in the future. [5]

The aim of this study was to evaluate the effects of FASN inhibition using the compound UCMG028, a candidate FASN targeting anticancer agent. For this

purpose, incubation of the ovarian cancer cell line SKOV3 with this compound was performed and cellular events taking place in response to this treatment were determined using proteomics and metabolomics approaches. Comparison of treated and non-treated ovarian cancer cells using proteomics approaches enabled us to assess proteomic changes occurring after FASN inhibition corresponding to cell cycle and cell growth arrest, and induction of apoptosis. Since the targeted enzyme is involved in fatty acid synthesis, the expected decrease in its activity was verified with a targeted metabolomics assay using multiple reaction monitoring (MRM); the aim was to determine the decrease of fatty acid products such as acylcarnitines, as well as phospho- and sphingolipids. Furthermore, although a direct correlation between inhibition of fatty acid synthesis and amino acid metabolism has not been verified until now, a comparison of the amino acid- and biogenic amine concentrations before and after FASN inhibitor treatment were also made, in order to detect possible perturbations related to amino acid metabolism.

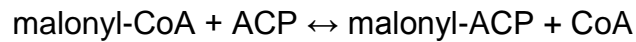
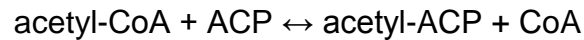
1.2 Fatty acid biosynthesis [6]

Phospholipids are essential components of cellular membranes. A phospholipid molecule consists of four components: one or more fatty acids, a basic molecule (glycerol or sphingosine) to which the fatty acids are coupled, a phosphate group and an alcohol attached to it. Phospholipids may carry fatty acids with various chain length and degree of saturation. Fatty acid biosynthesis occurs in the cytoplasm and begins with the formation of palmitic acid - a saturated fatty acid with a chain length of 16 carbon atoms - which is the precursor of all fatty acids. Its synthesis begins with the carboxylation of acetyl-coenzyme A (CoA), which results in formation of malonyl-CoA. This reaction is catalyzed by the acetyl-CoA-carboxylase which carries biotin as a prosthetic group. During this reaction, a carboxybiotin intermediate is built by using an ATP molecule. The activated CO₂ group is then transferred to acetyl-CoA:

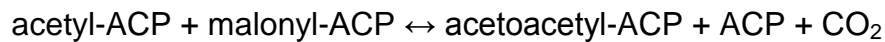


The so formed malonyl-CoA serves as a precursor for the synthesis of saturated long chain fatty acids. Prolongation of the fatty acid chain with two carbon atoms is performed by a series of reactions (condensation, reduction, dehydration and reduction), catalyzed by the fatty acid synthase (FASN). The condensation occurs via reaction with an acetyl-CoA molecule, while for the reduction steps an NADPH molecule is used. All intermediates are attached to acyl carrier proteins (ACPs), where coenzyme A serves as a linker between the fatty acid intermediate and a serine residue of the acyl carrier protein. Thus, the prolongation phase begins with

the formation of acetyl-ACP and malonyl-ACP, catalyzed by the acetyl transacylase and the malonyl transacylase, respectively:



This is followed by a reaction between acetyl-ACP and malonyl-ACP resulting in formation of acetoacetyl-ACP:



In this condensation step a carbon chain of four carbon atoms is formed of two carbon chains with the length of two and three carbon atoms respectively. This is accompanied by the release of a CO₂ molecule. It is to be noticed that the use of an ATP molecule is essential for the condensation reaction. ATP is involved in the formation of malonyl-CoA whose free enthalpy is released after reaction with acetyl-ACP.

In the next three steps of the fatty acid prolongation, the carbonyl group on the C-3 atom of the fatty acid chain is reduced to a methylene group. Acetoacetyl-ACP is first reduced to D-3-hydroxybutyryl-ACP with the aid of NADPH as a reducing agent, followed by a dehydration step to crotonyl-ACP. This intermediate is then reduced using another NADPH molecule to form butyryl-ACP, which completes the first prolongation cycle of the fatty acid chain. Figure 1 shows a scheme of the reaction series described above.

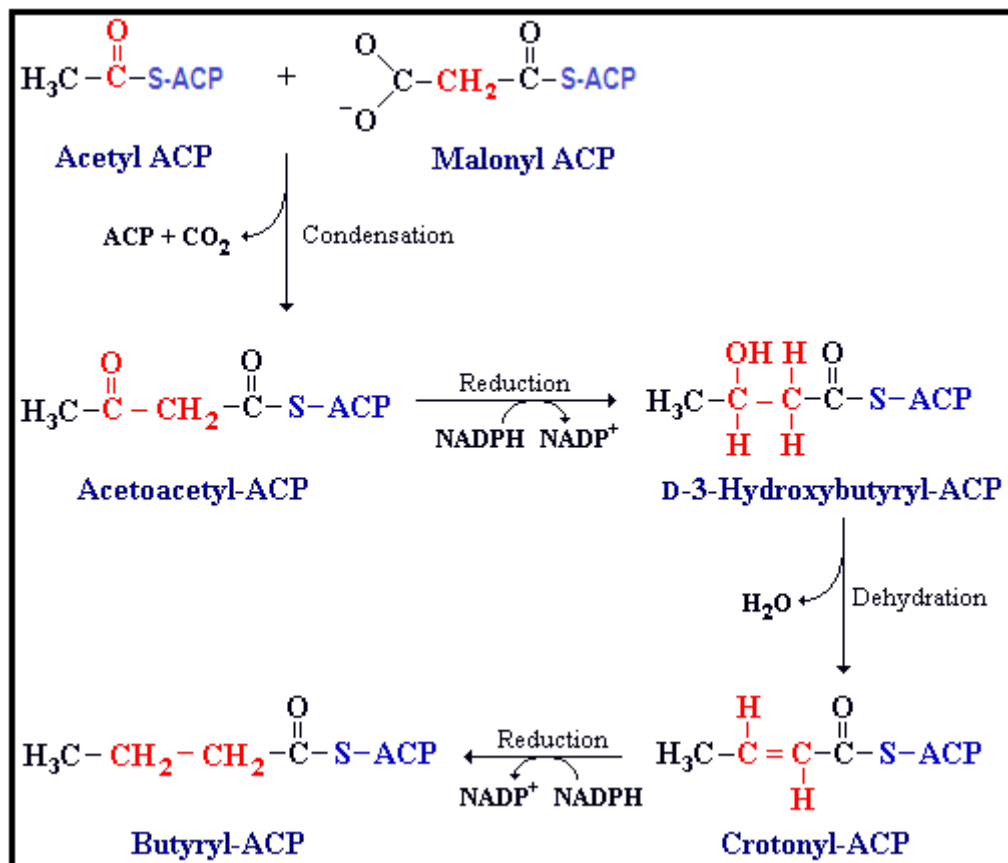


Figure 1. Prolongation of the fatty acid chain. The intermediates shown in this figure are formed in the first prolongation cycle of the fatty acid chain.

Butyryl-ACP is then used as a precursor for a second prolongation cycle by reacting with malonyl-ACP. Further reduction, dehydration and reduction steps convert the C_4 -ketoacyl-ACP in C_6 -acyl-ACP, which enters a third prolongation cycle. The prolongation fatty acid chain continues until the synthesis of C_{16} -acyl-ACP. This product is then hydrolyzed by the thioesterase to palmitic acid and ACP.

Further prolongation and desaturation of fatty acid chains is performed by several enzymes situated on the cytoplasmic side of the endoplasmic reticulum (ER). During prolongation of the fatty acid chain malonyl-CoA acts as a C_2 -donor. Fatty acid desaturations are catalyzed by enzyme complexes attached to the ER membrane, using oxygen and NADH (or NADPH).

1.3 Fatty acid synthase (FASN)

1.3.1 Structure and biological function [6]

Fatty acid synthase is a dimer of two identical 272 kDa subunits. The subunits consist of three catalytic domains, each one responsible for one of the corresponding reactions: condensation, reduction and palmitic acid release (see Figure 2). The domains are separated by flexible regions, enabling the cooperation between their active centers. Domain 1, the condensation unit, incorporates acetyl-transferase, malonyl-transferase, and β -ketoacyl synthase, and catalyses condensation of Acetyl-ACP and Malonyl-ACP. Domain 2 is the reduction unit, where the carbonyl group is transformed to a methylene group. It contains the acyl carrier protein, the β -ketoacyl reductase, the dehydratase and the enoyl reductase. Domain 3, the subunit for palmitic acid release, accommodates the thioesterase. In the course of a prolongation cycle the fatty acid chain is attached to a phosphopantetheine group, with the aid of which it is carried from one catalytic center to another. Although all enzymes needed for the fatty acid synthase are located in a single subunit, FASN is catalytically active only after formation of a dimer.

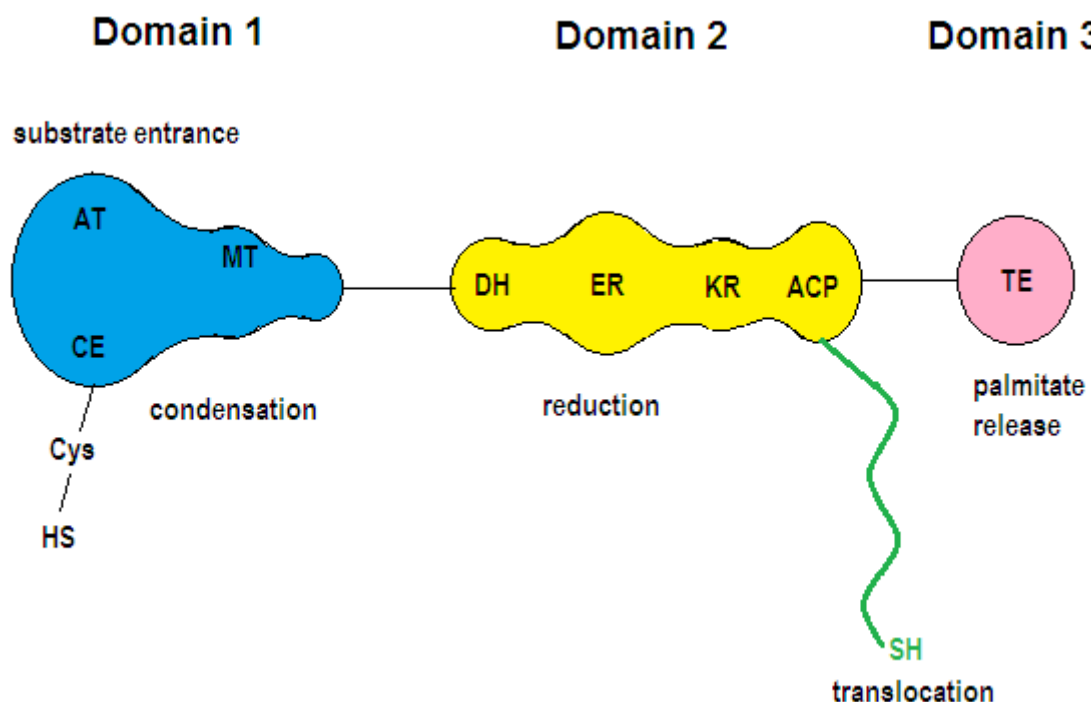


Figure 2. Schematic representation of a single fatty acid synthase chain. Domain 1 contains acetyl transferase (AT), malonyl transferase (MT) and the condensating enzyme (CE). In domain 2 the acyl carrier protein (ACP), the β -ketoacyl reductase (KR), the dehydrogenase (DH) and the enoyl reductase (ER) are incorporated. The thioetherase (TE) is located in domain 3. The phosphopantetheine group is represented in green.

1.3.2 Upregulation of FASN in cancer cells

The levels of FASN expression and activity in normal non proliferating cells is low (except for liver and adipose tissue [4]), since fatty acids are generally supplied by diet. [7] However, in rapidly proliferating cancer cells fatty acids can be synthesized *de novo* in order to provide lipids for membrane formation and energy supply via β -oxidation. Therefore, FASN is overexpressed in many tumors including prostate, ovarian, breast, malignant melanoma, neuroblastoma and retinoblastoma, multiple myeloma etc. [4] Figure 3 illustrates the mechanism of fatty acid biosynthesis in cancer cells.

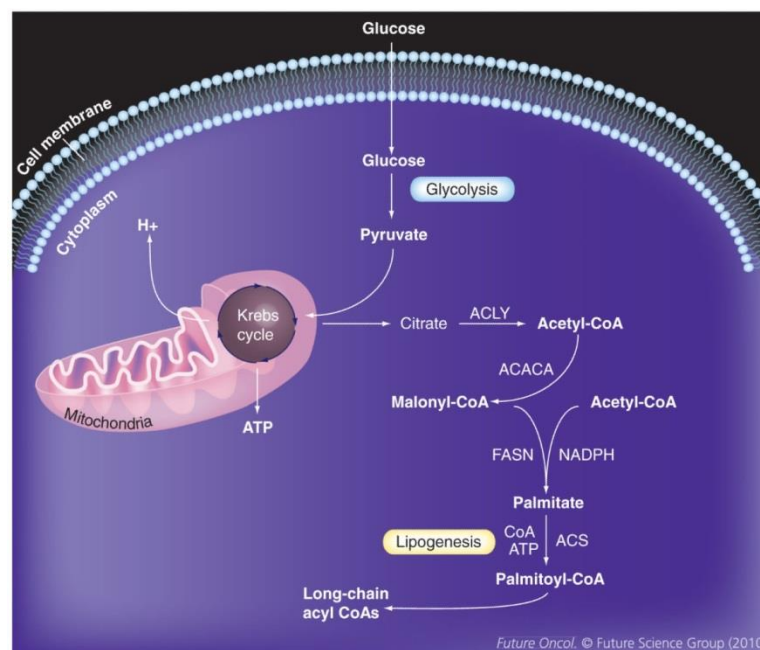


Figure 3. Fatty acid biosynthesis in a cancer cell. Excess of glucose is taken up and converted into pyruvate via anaerobic glycolysis. Pyruvate is then used in the Krebs cycle for production of ATP and citrate. Excess citrate serves for the formation of acetyl-CoA, which enters the lipogenesis pathway to produce long chain acyl-CoAs. (from [4])

The regulation of FASN in cancer occurs through complex mechanisms involving transcriptional and post-translational control combined with microenvironmental factors. One suggested mechanism causing FASN overexpression is through activation of growth factor receptors such as ErbB2 and EGFR by their corresponding ligands, leading to activation of the mitogen activated protein kinase (MAPK) and phospho-inositide 3-kinase (PI3K/AKT) signaling pathways, known to contribute to uncontrolled growth and resistance to apoptosis and therefore essential for tumor progression. [8] Both transduction pathways activate the transcription of FASN. Another way to activate AKT and MAPK in hormonally sensitive organs (e.g. breast,

endometrium, ovaries, prostate) is through activation of hormone receptors by estrogen, progesterone and androgen. Both signaling cascades modulate the expression of sterol regulatory element-binding protein (SREBP-1c), which binds regulatory elements in the FASN promoter. Protooncogene FBI-1 synergistically activates FASN-transcription by interacting with SREBP-1c. (Figure 4) It was evidenced in breast cancer epithelial cells that FASN, in turn, can activate the tyrosine kinase growth factor receptor, thereby setting up an auto-regulatory loop. Furthermore, degradation of FASN may be prevented by the ubiquitin specific protease 2a (USP2a), a pre-proteosomal deubiquitinating enzyme which can interact with and stabilize FASN through the removal of ubiquitin. USP2a is androgen regulated and overexpressed in prostate cancer. Its functional inactivation results in decreased FASN levels and induction of apoptosis. [4]

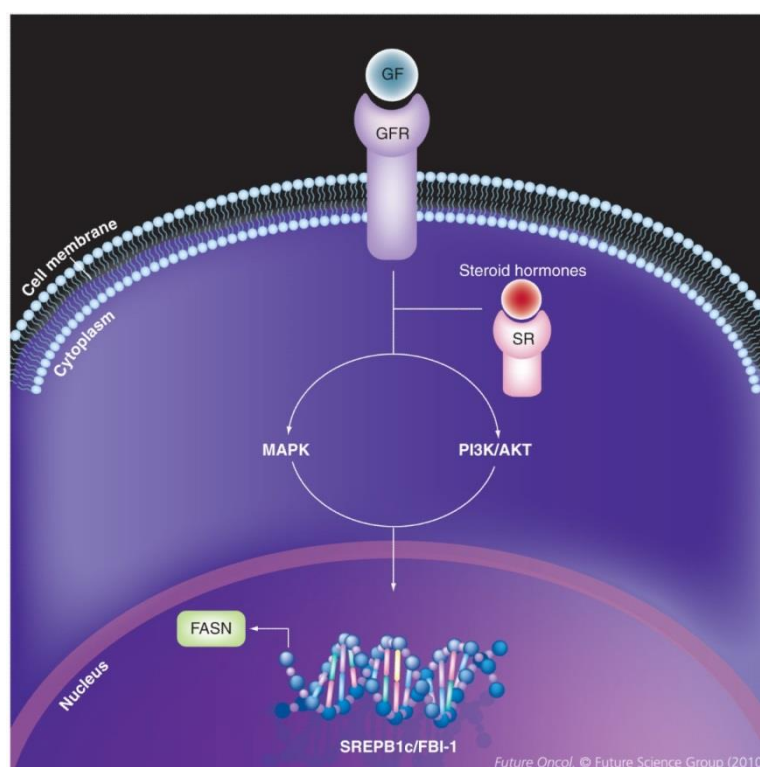


Figure 4. Regulation of fatty acid synthase expression in malignancy. Activated by either growth factor receptors or steroid hormone receptors, the MAPK and PI3K/AKT signaling cascades modulate the expression of SREBP-1c and FBI-1, which bind to regulatory elements in the FASN promoter. FASN: Fatty acid synthase; FBI-1: Pokemon; GF: Growth factor; GFR: Growth factor receptor; SR: Steroid Hormone receptor; SREBP-1c: Sterol regulatory element-binding protein 1c. (from [4])

As previously mentioned, FASN regulation can also be influenced by environmental stress. Futura *et al.* have demonstrated that the enzyme was significantly up-

regulated by hypoxia in breast cancer cell lines [4]. In their xenograft mouse model, FASN was strongly upregulated in the hypoxic tumor regions. In addition, immunohistochemical experiments in human breast cancer revealed that the expression of FASN and SREBP-1c are localized within hypoxic regions. [4]

1.3.3 FASN as a potential therapeutic target for cancer therapy

Recent studies on the role of FASN in cancer cells provide evidence that FASN is a promising target for therapy of several cancer types. Phospholipids generated by FASN are integrated into membrane lipid rafts which accommodate receptor tyrosine kinases including the epidermal growth factor receptor (EGFR, ErbB1) and ErbB2 (HER2/neu). Therefore FASN plays a critical role in the initiation of cell growth signaling. Studies on the interaction between fatty acid synthase and the ErbB system reveal that the FASN inhibitor C75 sensitizes ovarian cancer cells to anti-ErbB drugs, suggesting cooperation between both systems. Moreover qRT-PCR and Western blot assays show that FASN inhibition by C75 represses not only FASN, but also proteins involved in cell growth signaling (EGFR, ErbB2, and AKT). Interestingly, ErbB2 mRNA is not affected by C75 in the ovarian cancer cell line A2780. Nevertheless, a decrease of the amount of total and phosphorylated ErbB2 is observed, which rather supports a post-transcriptional regulation of growth factor receptors in ovarian cancer. [9]

Menendez *et al.* suggest three possible mechanisms of ErbB2 regulation induced by FASN inhibition (Figure 5) [10]:

- a. Disruption of fatty acid synthesis results in accumulation of malonyl-CoA, which triggers the up-regulation and nuclear accumulation of PEA3 able to repress the ErbB2 promoter. [10]
- b. FASN inhibition also causes NADPH accumulation that may activate reactive oxygen species (ROS) generating enzymes such as the NADPH-oxidase (NOX), which could lead to blockade of ErbB2 protein expression. [10] In general, the accumulation of reactive oxygen species and FASN substrates, as well as depletion of FASN end products can cause cell stress. Consequently, the malignant cells produce unfolded proteins, which is part of the endoplasmic reticulum stress response. As a result of these processes, cell growth can be inhibited. [11]
- c. ErbB2 clusters are accommodated into membrane lipid rafts which significantly influence the receptors biological function (tyrosine kinase activity). In addition, transport equilibrium of ErbB2 to and from the membrane is taking place. ErbB2 homodimers and ErbB2-containing heterodimers

undergo slow endocytosis and more frequently recycle back into the cell membrane. Blockade of FASN activity, affecting the synthesis of lipids that are essential for the formation of membrane lipid rafts, may negatively affect the localization of ErbB2 in the membrane of cancer cells and hence shut down its tyrosine kinase activity and the cell growth signaling cascade mediated by ErbB2. A shift in the ErbB2 transport equilibrium can cause ErbB2 endocytosis followed by lysosomal degradation. [10]

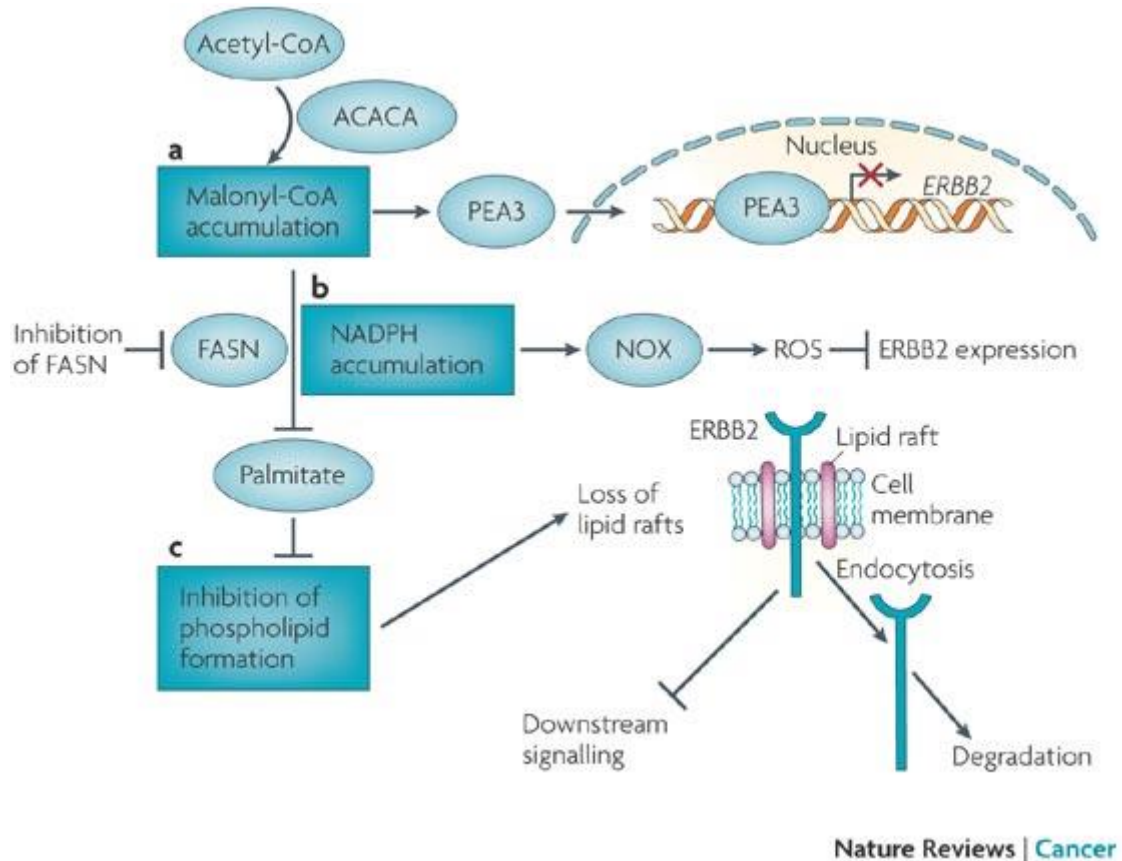


Figure 5. ErbB2 down-regulation induced by FASN inhibition a. Malonyl-CoA promoted transcriptional repression of ErbB2 b. NADPH-related induction of reactive oxygen species (ROS) c. Phospholipid-related subcellular compartmentalization of the ErbB2 network; ACACA: acetyl-CoA-carboxylase; PEA3: ETS translocation variant 4; FASN: fatty acid synthase; NOX: NADPH oxidase; ROS: reactive oxygen species; ErbB2: Receptor tyrosine-protein kinase ErbB-2 (from [10])

It should be noted, that the three suggested pathways might concurrently inhibit ErbB2 activity.

Other experiments in ovarian cancer cell lines show that FASN inhibition does not only abrogate lipogenesis, but also down-regulates oncogenic phosphoinositide-3-kinase (PI3K) signaling. [5] The PI3K signaling cascade plays a key role in many cellular functions including proliferation, differentiation, tumorigenesis, angiogenesis, autophagy and apoptosis. A significant part of ovarian carcinomas experience aberrant expression of proteins within the PI3K system, such as PI3K itself, AKT,

mTOR, and p70S6K; mTOR plays an essential role in cell growth and metabolism by regulating protein and RNA stability, transcription and mRNA translation. [12] It activates either ribosomal protein S6 or the translation initiation factor 4E (eIF4E) inhibitor-binding protein 1 (4EBP1). S6 is a component of the 40s ribosomal subunit, involved in protein synthesis, while 4EBP1 modulates the activity of eIF4E, which is required for translation of growth promoting genes. Hence, S6 and eIF4E are both involved in protein biosynthesis and cell growth. In addition, the PI3K pathway is able to transmit oncogenic signals derived from ErbB1 and ErbB2. It was found that inhibition of FASN by C75 or siRNA knockdown significantly increases the ubiquitination of protein members of the PI3K cascade. [5] Since the attachment of ubiquitin to a target protein usually induces its degradation, it is likely that FASN inhibition down-regulates oncogenic signaling by inducing proteolysis of PI3K signaling proteins. [4] This statement is corroborated by the finding that FASN activity is inversely related to the expression of several ubiquitinating enzymes. [5]

Furthermore, inhibition of FASN by C75 in epithelial ovarian carcinoma (EOC) causes inhibition of cell viability by inducing apoptosis via the mitochondrial pathway. Experimental evidence suggests that the apoptotic pathway is activated by disruption of the mitochondrial membrane, allowing activation of proapoptotic proteins and release of cytochrome c into the cytosol. Released cytochrome c interacts with the apoptotic protease-activating factor 1 (APAF1) and caspase 9, which results in formation of apoptosomes, with subsequent activation of caspase 3. This mechanism is clearly induced by inactivation of serine/threonine-protein kinase (AKT), observed after treatment of EOC cells with C75 and gene silencing of FASN. As already mentioned, AKT is a regulator of cellular processes including proliferation, cell survival, growth and angiogenesis. [12] It is known that its inactivation induces apoptosis via the mitochondrial pathway. [7]

Successful treatment of cancer cell lines with therapeutic agents in combination with FASN inhibitors was also reported. Such combinatory therapeutic strategies might be successful in treating malignancies showing chemoresistance to currently used anticancer drugs. Treatment of EOC xenograft tumor in mice with a combination of subtoxic doses of C75 and cisplatin shows a significant reduction in the tumor size and weight in mice in comparison to treatment with C75 or cisplatin alone. As a conclusion, the combination of a FASN inhibitor with a conventional anticancer agent may be more effective for the treatment of certain tumor types. [7]

Fatty acid synthase is also believed to regulate aggressiveness in ovarian cancer cells. Increased FASN levels were associated with a significant increase of tumor burden (number of tumor cells) in the peritoneal metastasis of ovarian cancer accompanied by enhancement of cellular colony formation and metastatic ability. Conversely, FASN knockdown using RNA interference shows reduction of ovarian cancer cell migration *in vitro* and peritoneal dissemination *in vivo*. Further studies suggest that overexpressed FASN is involved in induction of epithelial-mesenchymal transition (EMT) via transcriptional regulation of *E*-cadherin and *N*-cadherin. EMT is

one of the mechanisms which help cancer cells to acquire invasive and metastatic abilities. It enables an epithelial cell, characterized by a rather immobile state due to its interaction with a basement membrane via its basal surface, to transform into a mesenchymal cell characterized by elevated migratory capacity, invasiveness, increased resistance to apoptosis and increased production of extracellular matrix (ECM) components. During EMT, the underlying basement membrane of the cell is degraded and the formed mesenchymal cell is free to move away from the epithelial layer from which it originates. Furthermore, the expression of *E-cadherin* is down-regulated, while the expression of *N-cadherin* increases, which promotes interaction with endothelial and stromal components. Zhang *et al.* have demonstrated that this process is promoted by FASN via inhibition of the activity of the *E-cadherin* promoter with simultaneous enhancement of the activity of the *N-cadherin* promoter. (Figure 6) [2]

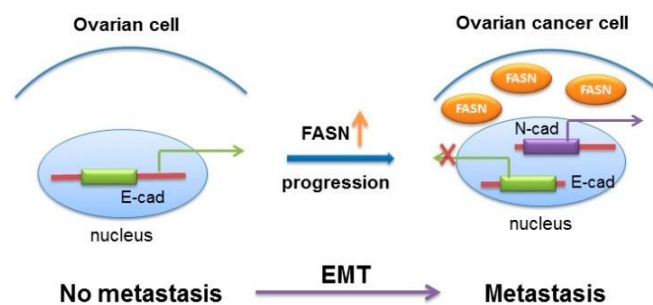


Figure 6. Mechanism of FASN controlling EMT in ovarian cancer (from [2])

For a complete understanding of the role of FASN in EMT initiation in tumor cells, a more detailed mechanism of the transcriptional regulation of *E-cadherin* and *N-cadherin* has to be elucidated in the future. [2]

According to a widely accepted theory, normal ovarian cells do not express FASN and are therefore insensitive to FASN inhibitors. However, a recent cell culture study about FASN expression in normal non-malignant human ovarian surface epithelial cells controverts this notion by demonstrating that normal proliferating ovarian cells do produce high amounts of FASN and are FASN inhibitor sensitive. In contrast to that, normal ovarian cells residing in their autochthonous tissues induce senescence, which leads to down-regulation FASN, and these cells are resistant to FASN inhibitors. However, an important difference of normal ovarian cells in comparison to ovarian cancer cells is that in healthy proliferating cells FASN inhibitors cause only a deceleration in the cell duplication rate, while cancer cells show cell cycle blockage and apoptosis. A possible explanation for this observation may be that repair and gatekeeper systems such as the INK4A/Arf/p53/pRb-pathway are only affected in ovarian carcinoma cells. As a consequence, ovarian cancer cells are susceptible to metabolic stress induced toxicity as caused by phospholipid deprivation. This contrasting behavior of normal and cancer cells towards FASN inhibition implies that

a FASN targeted cancer therapy selective for ovarian cancer cells can be developed without causing adverse side effects. [1]

1.3.4 FASN inhibitors

To date, several compounds have been reported to inhibit the activity of fatty acid synthase, including cerulenin, C75, orlistat, C93 and naturally occurring polyphenols (see Figure 7).

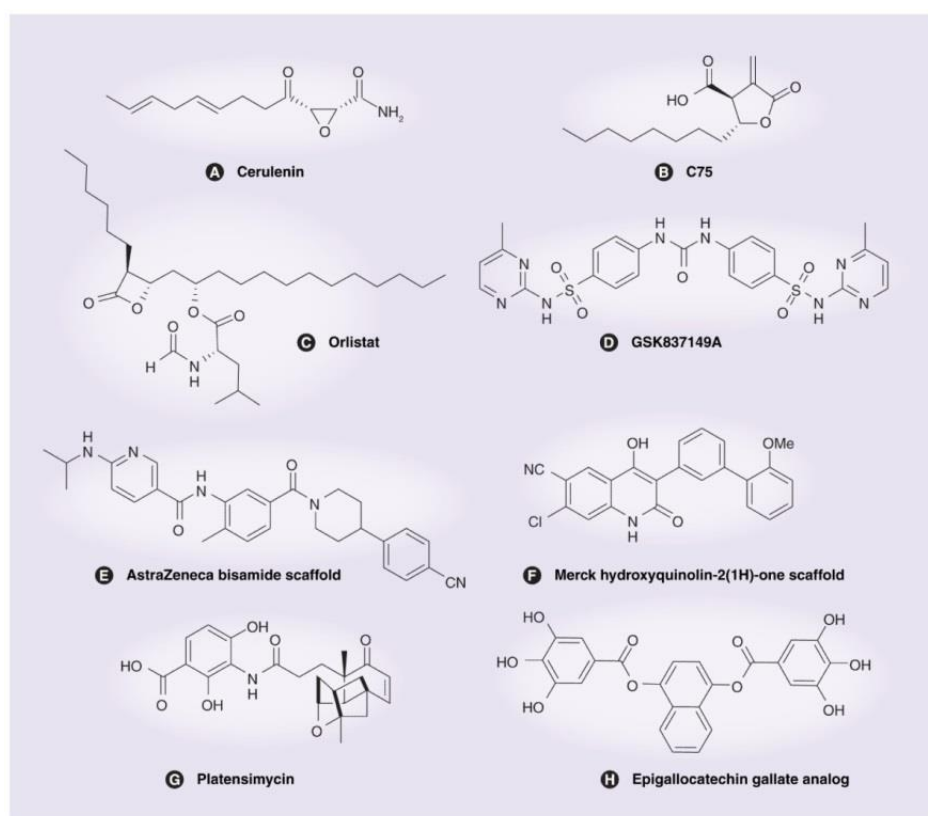


Figure 7. Structural formulas of fatty acid synthase inhibitors (from [4]) **(A)** Cerulenin. **(B)** C75. **(C)** Orlistat. **(D)** GSK837149A. **(E)** AstraZeneca bisamide scaffold. **(F)** Merck hydroxyquinolin-2(1H)-one scaffold. **(G)** Platensimycin. **(H)** Epigallocatechin gallate analog.

Cerulenin and C75 are early, small-molecule inhibitors, both known as effective antitumor agents. Cerulenin, a natural product isolated from the bacterial strain *Cephalosporium caerulens* has an epoxy group that reacts with the ketoacyl synthase domain of FASN (see Figure 2). It was one of the first compounds demonstrating an antitumor activity in breast cancer cell lines, inducing apoptosis and inhibiting tumor progression in a xenograft model of ovarian cancer.[4] C75 is a cerulenin derivative, developed to overcome the chemical instability of cerulenin. It

interacts with β -ketoacyl synthase, the enoyl reductase and the thioesterase domains and inhibits FASN in an irreversible manner. Tumor growth inhibition in xenograft breast cancer models and a chemopreventive activity for mammary cancer in neu-N transgenic mice was observed after treatment with C75. Despite their significant antitumor activity, these compounds cause severe side effects in food intake and body weight in mice, which impedes their further development as therapeutic agents. Recently, more potent FASN inhibitors were designed based on C75. [4]

Several natural plant-derived polyphenols have also been shown to inhibit FASN. Epigallocatechin-3-gallate (EGCG), a natural component of green tea is the best characterized polyphenole agent. However, EGCG is a promiscuous agent targeting different signaling cascades. [4]

Orlistate is a US FDA-approved pancreatic lipase inhibitor, originally developed as an antiobesity drug, showing an antiproliferative activity in prostate cancer cell lines and tumor growth inhibition in a xenograft prostate cancer model. Published co-crystal structures show that orlistat blocks FASN activity in an irreversible manner by forming a covalent adduct with the active serine of its thioesterase domain. Despite its potency, this compound suffers from several limitations, hampering its clinical use: low cell permeability, low solubility, lack of selectivity, poor oral bioavailability, and poor metabolic stability. Several orlistat analogues have been synthesized in order to improve these limitations. [4]

Recently, several novel FASN blockers have been developed and are now subjected to clinical evaluation. C93, designed to overcome C75's lack of potency and side effects is among these promising agents. It has shown significant tumor growth arrest in lung cancer and ovarian cancer xenograft models. [4] Importantly, no weight loss was observed during treatment with C93. Furthermore, the vitamin-D2 derivative MT19c was also reported to down-regulate FASN activity both in *in vivo* and *in vitro* models of ovarian cancer. Unlike previously synthesized vitamin-D derivatives, MT19c did not show hypercalcemic side effects. [13]

1.4 Proteome profiling

1.4.1 Definition and goals of proteome profiling

Proteomics is the analysis of the proteome of a cell aiming to investigate biological processes [14]. Typically, proteomics experiments shall lead to the comprehensive description of gene expression in a given cell type and alterations caused by intracellular and/or extracellular stress [14]; interactions between proteins involved in specific processes and pathways inside the cell might be elucidated as well by proteomics [15]. These goals require involvement of various disciplines such as

molecular biology, bioinformatics and biochemistry. In addition, various tools can be utilized along the proteomics workflow: pre-separation of the proteome by 1D gel electrophoresis, protein digestion with trypsin, protein identification/quantification by high resolution MS instruments and subsequent data processing and analysis using bioinformatics tools [15].

1.4.2 Methods and tools of proteomics

1.4.2.1 Mass spectrometry based shotgun proteomics

Shotgun analysis is a commonly applied strategy for the analysis of complex protein mixtures. [16] A schematic view of an exemplary workflow of a shotgun proteomics assay is illustrated in Figure 8. In this technique, the protein mixture isolated from a biological sample (e.g. cell culture) is converted into a peptide mixture via protein digestion. For this purpose, trypsin is the most frequently used enzyme. [17] Trypsin is a serine protease, which catalyzes the cleavage of peptide bonds at the C-terminus of arginine and lysine, both basic amino acids. For higher digestion efficiency, trypsin can also be used in combination with a second protease such as Lys-C, which has a high activity and specificity for lysine residues and, unlike trypsin, can cleave lysines followed by prolines. The use of a trypsin/Lys-C mix improves protein digestion by eliminating the majority of missed cleavages typically observed after digestion with trypsin alone, thus providing an increased number of identified peptides and proteins, an improved reproducibility and a more accurate protein quantitation. [17]

Usually, there exist two different types of workflows for protein digestion: a gel electrophoresis-based and a gel-free (or in-solution based) method. In the gel electrophoresis-based approach, the protein mixture is at first separated in one or two dimensions (1D/2D) prior to in-gel enzymatic digestion. In the second approach, the protein mixture is digested in-solution, without pre-separation of the proteins according to their molecular weights. Thus, the in-solution based technique tends to be simpler and less time consuming. Conversely, in-gel digestion provides complexity reduction on the protein level, allowing identification of a larger number of proteins. Moreover, all contaminants (e.g. detergents, salts) are removed during electrophoresis and the generated peptide samples are ready for (LC-) ESI-MS/MS analysis. Limitations of this procedure can arise from poor accessibility of the protease to target proteins in the gel and/or inefficient release of peptides from the gel matrix. [18]

After obtaining a peptide mixture, the sequences of the produced peptides are analyzed. For this purpose, peptides must be separated efficiently from each other

prior to peptide sequence analysis. High performance liquid chromatography (HPLC) is the most widely established separation technique for complex peptide mixtures. The stationary phase used for LC separation is usually reverse phase (RP). Peptides interact with a hydrophobic stationary phase in the presence of a polar hydrophilic mobile phase. Hence, the peptides are separated according to their relative hydrophobicity with the most hydrophilic analytes eluting earlier in the LC run. [18]

After chromatographic separation, peptide sequencing is performed via tandem mass spectrometry in which, after analyte fragmentation using e.g. collision induced dissociation (CID), peptide sequences can be determined from the MS/MS fragmentation pattern. Amino acid sequences are determined by analysis of the fragment ion series obtained from the MS/MS spectrum, assuming that the mass difference between neighbouring signals within a series is equal to the mass of one amino acid. [19]

Finally, protein identification occurs by adjusting the obtained peptide sequences to protein sequences obtained from *in-silico* digestion of all known proteins, using bioinformatics tools. [19] This can be achieved using the Basic Local Alignment Research tool (BLAST) which compares protein sequences to sequence databases and calculates the statistical significance of matches. [20]

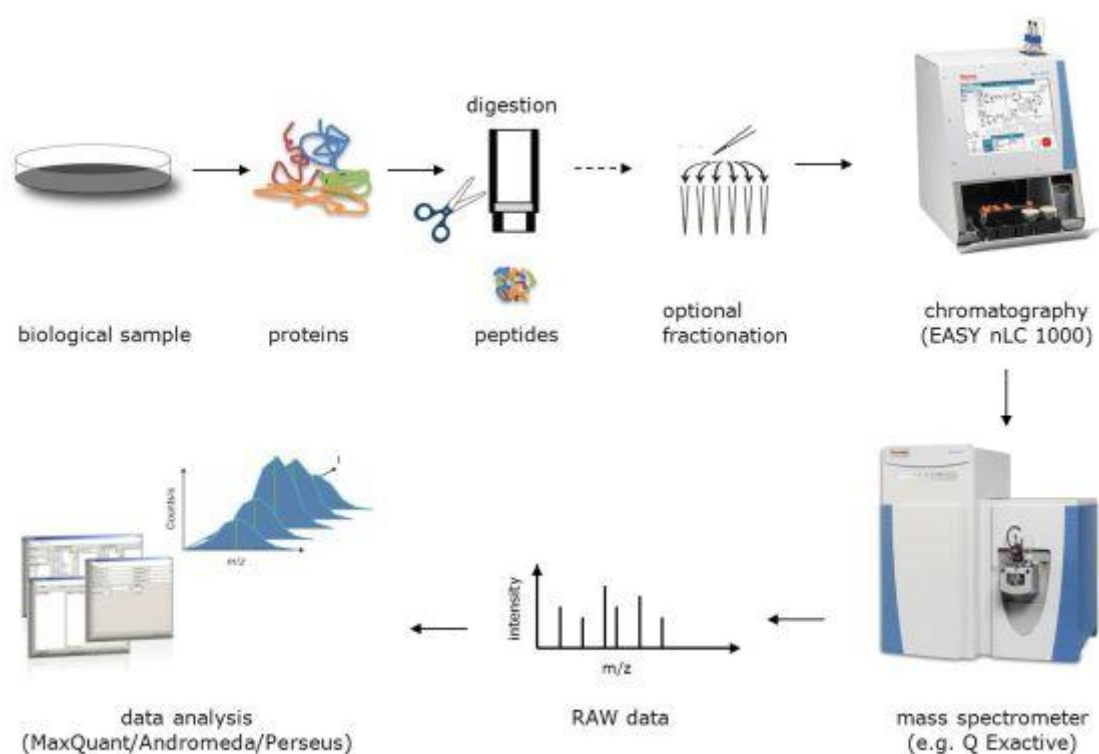


Figure 8. Typical workflow of a shotgun proteomics assay (from [21])

1.4.2.2 Q Exactive Orbitrap Mass Spectrometer

The Q Exactive hybrid quadrupole orbitrap mass spectrometer consists of an electron spray ionisation (ESI) source, S-lens, a bent flatapole, a quadrupole mass filter, a C-trap, a high energy collisional dissociation (HCD) cell and an orbitrap (Figure 9). [22]

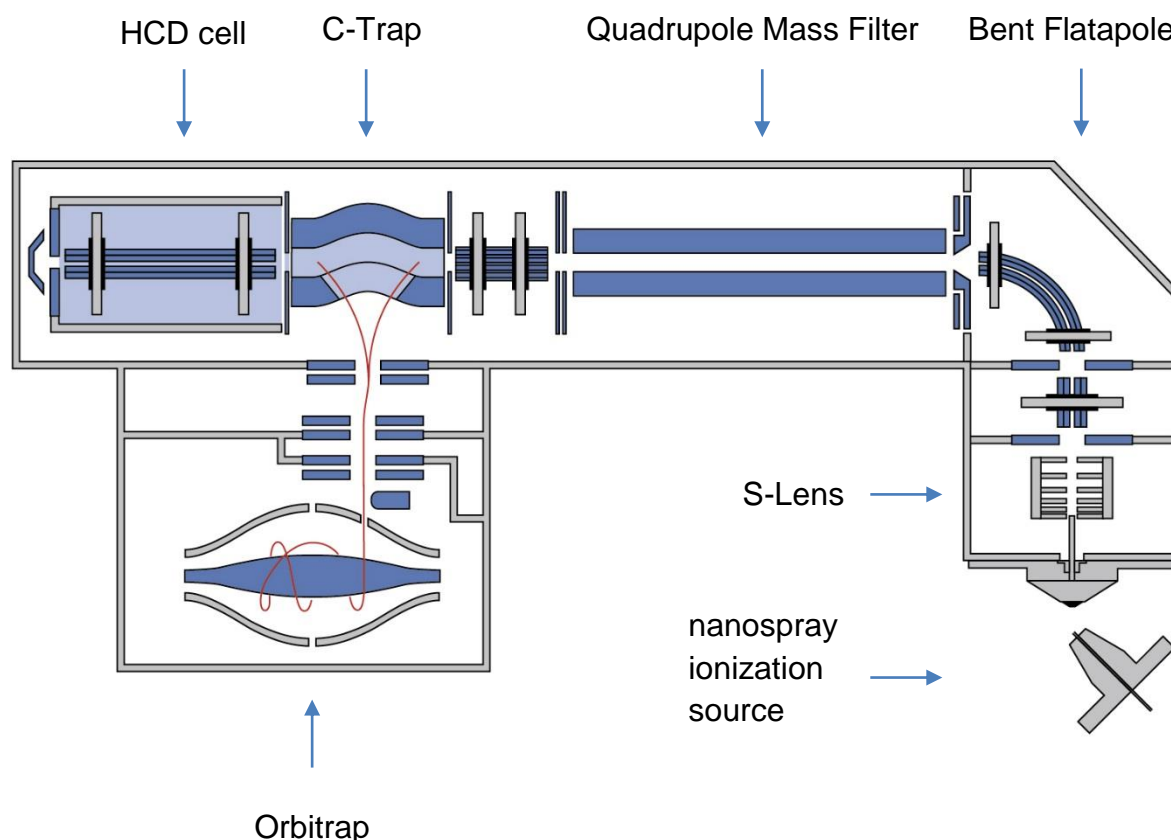


Figure 9. Schematic diagram of a Q Exactive orbitrap instrument (from [23])

The ion beam arising from the nanospray ionisation source is first focused through the S-lens, followed by elimination of all neutral species in the bent flatapole [26]. The quadrupole mass filter selects ions of a defined mass range, which are then accumulated in the C-trap and fragmented in the HCD cell. Another role of the C-trap is to compress the ion population prior to injection in the orbitrap analyser. Finally, the m/z values of the obtained fragment ions are derived from their oscillation frequencies along the axis of the orbitrap [24], estimated by an image current detection and a fourrier transformation (FT) algorithm [25].

Common features of the orbitrap mass analyser are high mass accuracy, large dynamic range and low detection limits. The combination with a quadrupole mass filter improves the sensitivity for MS/MS measurements, since a pre selection of ions with m/z values within the analyte mass range can be performed. In addition,

simultaneous ion filling/fragmentation and orbitrap detection increases the acquisition speed of the instrument [26]. Therefore, coupled with an HPLC system, the Q Exactive mass spectrometer is suitable for analysis of complex biological samples such as proteome profiling.

1.4.2.3 Max Quant

Max Quant is a set of algorithms, which uses information from raw MS data for protein identification and quantification. In each MS spectrum peaks are detected by fitting a gaussian peak shape. Incompletely separated peaks are split by significant local minima. Furthermore, the centroid mass of each 2D peak is calculated, which provides an accurate, intensity weighted estimate of the peptide mass. The 2D peaks of adjacent MS scans are gathered to obtain three-dimensional (3D) peak hills over the retention time. In this process, two peaks in neighboring spectra are connected when their centroid masses are significantly close. The obtained 3D peak is quantified by integration of its intensity. For determination of isotope patterns, an edge is inserted between two peaks when the mass difference equals the difference in isotope mass of an average amino acid, and when the intensity profiles have a sufficient overlap in their retention times. Isotope patterns reduce data sets tenfold and can serve as noise filters. An example of 3D peak detection is illustrated in Figure 10. [27]

The peptide and protein identification for label free experiments is performed with conventional database search, where the peptide sequences are identified by comparison of their MS or MS/MS mass values with calculated peptide mass or fragment ion mass values. [28] The obtained peptide hits are then assembled into protein hits. With the help of MaxQuant, a comparison of a particular protein amount in different proteomes is possible by calculating a protein ratio as the median of the ratios of all peptides belonging to the protein of interest. [27]

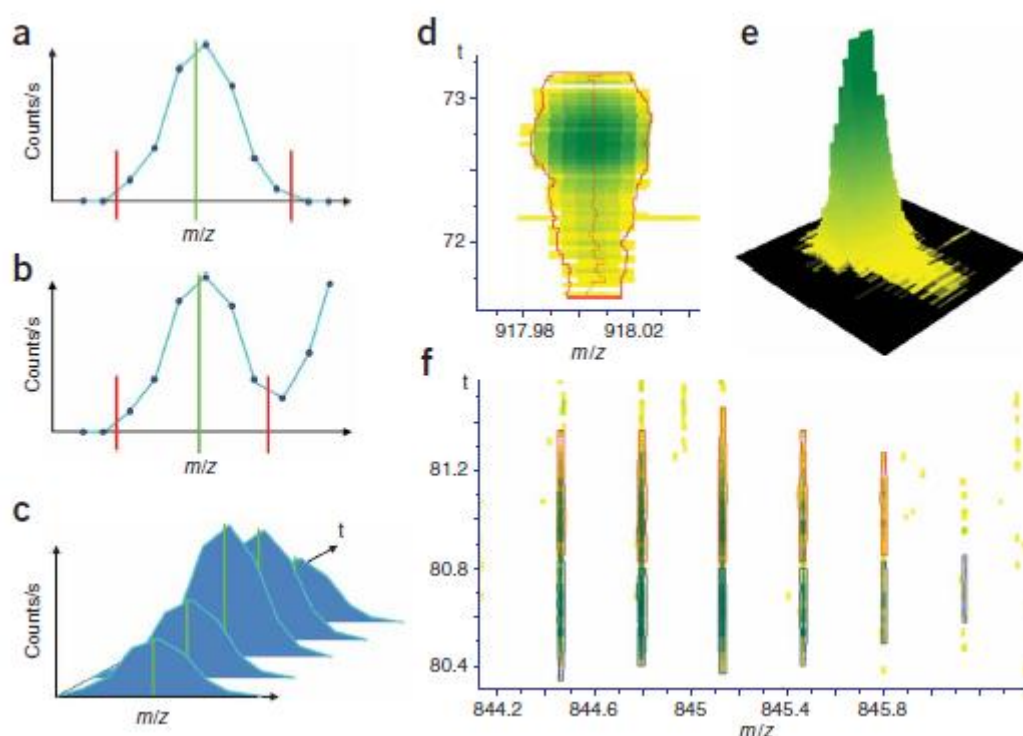


Figure 10. 3D peak detection using Max Quant (from [27])

- a) Two dimensional peak, whose intensity drops to zero on both sides
- b) Two peaks broken up at their local intensity minimum
- c) Assembling of two dimensional peaks from adjacent MS scans
- d) The resulting 3D peak presented with color-coded intensity, decreasing from green over yellow to white
- e) 3D representation of the same peak
- f) 3D peaks forming isotope patterns

1.5 Metabolomics

1.5.1 Definition and goals of metabolomics

The metabolome of a biological system represents the sum of all metabolites present in this system. Metabolomics assays aim to characterize the metabolic composition of a biochemical phenotype or a biochemical state. The analyzed species of a metabolic assay are low molecular, non-polymeric organic metabolites (e.g., amino acids, monosaccharides, biogenic amines, lipids, acylcarnitines). [19] Changes in the metabolome or in a specific metabolite are a direct result of activity changes of a protein or enzyme. Since the change in expression of a gene or protein does not necessarily correlate with a change in protein activity, proteomics and genomics

studies cannot fully characterize the state of a cell or biological system. In contrast with that, direct measurements of changes in the metabolome capture how biological systems respond to environmental and genetic stress. The exposure of a cell or tissue to a drug, for example, is expected to perturb the respective metabolome. [30]

The metabolome of a biological sample can be investigated with the aid of two distinct approaches: targeted and untargeted metabolomics. A targeted metabolomics assay aims to verify whether the expected cellular response has taken place after exposure to a certain type of cell stress (e.g., drug treatment, disease state, genetic modification). This is achieved by quantifying a specific metabolite or group of metabolites, as well as monitoring up- or down-regulations of those upon induction of environmental stress. Untargeted metabolomics is more discovery-based, meaning that the metabolites and the metabolic pathways affected by stress factors are unknown before analysis. Therefore, the objective of untargeted metabolomics is to monitor the entire metabolome in order to identify the affected metabolites and pathways. [30]

1.5.2 Targeted metabolomics using multiple reaction monitoring (MRM)

For the analysis of metabolite mixtures in complex biological matrices, a method providing efficient separation of the sample components followed by reliable identification and accurate quantification of each analyte is required. Reversed phase high performance liquid chromatography (RP-HPLC) is a widely used separation technique, as it allows the separation of compounds of a wide range of polarity by either isocratic or gradient elution. For a high number of analytes, a gradient elution profile is more suitable due to the overall faster analysis and better resolution. [31] In order to efficiently separate amino acids and biogenic amines from each other, a derivatization prior to chromatographic separation is often performed. The hydrophobicity of amino acids can be considerably increased by coupling aromatic residues to their amine groups, which increases the interaction with the hydrophobic stationary phase, and thus improves chromatographic separation. [19]

An alternative technique to HPLC-MS/MS is the flow-injection analysis coupled with tandem mass spectrometry (FIA-MS/MS), which uses a well-characterized analyte band in a flowing solvent stream. The high throughput, the fast analysis rate, the minimal sample consumption, and the ease of design and operation have made FIA to a popular sample introduction and online pretreatment technology. [31]

The identification of each metabolite can be performed with high specificity by using a hybrid mass spectrometer. The triple quadrupole mass spectrometer is the first instrument allowing not only isolation of selected species by their m/z value but also an additional analysis of their structure, by induction of fragmentation spectra. Different types of MS/MS analyses can be performed on the triple quadrupole mass

spectrometer, helping to resolve different scientific problems. For a high selective and high sensitive screen of multiple analytes, a multiple reaction monitoring (MRM) assay can be used. During MRM, quadrupole 1 (Q1) transmits only a set of selected m/z ranges, corresponding to the m/z ranges of the targeted analytes. The filtered species are then fragmented in quadrupole 2 (Q2) via collision induced dissociation (CID) with a collision gas (N, He or Ar), followed by selection of only signature fragment ions by Q3, which are then used for analyte identification and quantitation. [19] Figure 11 shows a scheme of a triple quadrupole performing an MRM assay.

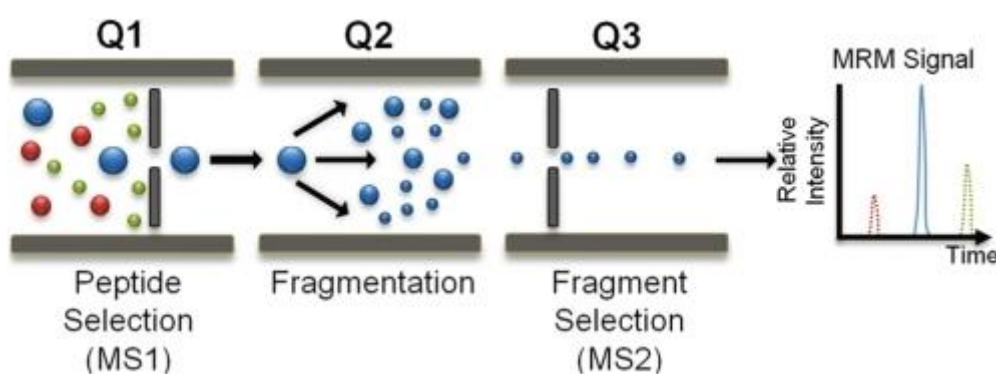


Figure 11. Multiple reaction monitoring mass spectrometry (MRM-MS) using a triple quadrupole mass spectrometer. (from [32])

2 Methods

All materials, reagents and stock solutions used are listed in the Appendix.

2.1 Cell culture experiments

The SKOV3 cells and the cell culture medium were provided by Univ.-Prof. Mag. Dr. Thomas Grunt from the Medical University of Vienna.

2.1.1 Preparation of the cell culture medium

The L-glutamine solution (200mM), the fetal bovine serum (FBS) and the penicillin-streptomycin solution (100x) (all stored at -20°C) were defrosted in a water bath at 37°C. The L-glutamine solution was placed in the ultrasonic bath and stirred until a clear solution was obtained. The fetal bovine serum was heated to 55-57°C in a water bath for 30 min under constant stirring. The fetal bovine serum was then added to the α -MEM cell culture medium. In addition, 5ml of the L-glutamine solution and the penicillin-streptomycin solution were added to the medium (100fold dilution). Final concentrations: 2mM L-glutamine, 10% FBS, 100 units/ml penicillin G, 0.1mg/ml streptomycin. The produced cell culture medium was stored at 4°C.

2.1.2 Cell culture and characterization of SKOV3 cells

10 ml of the prepared cell culture medium was pipetted in a cell culture flask (75cm²) and placed in the incubator for 30 min (temperature: 37°C, CO₂: 5%, air humidity: 95%). The cell line SKOV3 (stored in liquid nitrogen, passage number 513) was defrosted in a water bath at 37°C and transferred to the cell culture medium. The suspension was well mixed and the number of cells was estimated with a cytometer for which 10 μ l of the cell suspension were used. The cell concentration (cells/ml) was obtained by multiplying the cell number estimated in 10 μ l by 100 (estimated cell concentration: 6.05·10⁴ cells/ml). The cells were further cultivated in the incubator until confluence was achieved. The cell medium was exchanged with a fresh one by the following procedure: The cell culture medium (see section 2.1.1) was first placed in a water bath at 37°C for 30 min. The old medium was removed from the flask and replaced by 10ml of pre-warmed medium. The solution was well mixed and placed in the incubator. The achievement of cell confluence was monitored by observation under a microscope. These cells were harvested as described in section 2.2.1 and, subsequently, analyzed by shotgun proteomics using in-gel digestion (see section 2.3.1) and LC-MS/MS analysis with a QExactive orbitrap (see section 2.3.3)

2.1.3 Cell culture preparation for FASN inhibitor experiments

For the shotgun and targeted metabolomics experiments, three biological replicates were prepared for each of the four cell states (control 8h, control 24h, cells treated for 8h with FASN inhibitor, cells treated for 24h with FASN inhibitor). For proteome profiling, the cells were maintained in 25cm² cell culture flasks (12 flasks in total), while for the targeted metabolomics assay, cells were cultivated in two 6 well plates (one well plate for each incubation time - 8h and 24h). The cells were cultivated in the medium prepared for SKOV3 (see section 2.1.1) and observed under the microscope until confluence was reached. The final cell number in each cell culture flask was between 1 and 2 million, in each well between 0.5 and 1 million.

2.1.4 Incubation with UCMG028

The FASN inhibitor solution (UCMG028, MW: 464.38 g/mol, 20mg/ml, solved in DMSO), stored at -80°C in the dark, was defrosted at 4°C. The inhibitor solution was diluted to the ratio of 1:1000 in the cell culture medium (preparation see section 2.1.1), previously heated to 37°C. The final inhibitor concentration in the medium was therefore 0.02 mg/ml, the final DMSO concentration 0.1%. For the control group, a solution of 0.1% DMSO in the same cell culture medium (37°C) was prepared. All cell culture flasks and 6 well plates (see section 2.1.3) were removed from the incubator and media were exchanged with the inhibitor containing media or pure DMSO containing media, respectively (5ml in each T25 flask and 2,5ml in each well). For each incubation time (8h and 24h), three biological replicates both for controls and treated cells were prepared. The cells were then incubated in the dark (incubating conditions described in section 2.1.2).

2.2 Harvesting of cells

2.2.1 Harvesting of cells and preparation of protein extracts from cell cytoplasms and nuclei for proteomics experiments

For cell harvesting, the cell medium was removed and the cells were washed twice with 12ml of PBS buffer. The cell culture flask was then placed on ice. Thirty microliter of a 100mM phenylmethanesulfonylfluoride (PMSF) and a proteasome inhibitor cocktail (PIC) solution were added to 3ml (for T75 flasks) or 1ml (for T25 flasks) of isotonic lysis buffer (final concentrations: 1% PMSF, 1% PIC). The lysis buffer was pipetted in the cell culture flask followed by scraping off the cells from the bottom of the flasks. The cell suspension was transferred into a falcon. The disruption of the cytoplasm occurred by pressing the cell suspension eight times through a syringe against the falcon wall. The nuclei were centrifuged (4°C, 3500rpm, 5min, acceleration 9, deceleration 9) and the supernatant (cytoplasm fraction) was pipetted

in a falcon filled with 12ml of ice cold ethanol (final sample volume five times larger than the volume of the lysis buffer). The nuclear pellet was somewhat dried using a pulp, and 100 μ l of ice cold TE_{NaCl} solution containing 1% PMSF and 1% PIC was added, followed by disruption of the nuclei by pipetting the suspension through a 200 μ l pipette. Pipetting was repeated as often as required until the whole pellet was solved. The solution was placed on ice for 10 min, 900 μ l of TE_{NP40} containing 1% PIC and 1% PMSF was added and the solution was placed on ice again for 15 min. The sample was centrifuged (same parameters as described above) and the supernatant was transferred into a falcon filled with 4ml of ice cold ethanol (final sample volume five times larger than the volume of the lysis buffer). The proteins from both fractions were precipitated at -20°C overnight.

The samples were centrifuged (30 min, 4°C, 5000 rpm, acceleration 9, deceleration 4) and the supernatants were discarded. The protein pellets were let dry in the air and under vacuum in a desiccator (10min for the nucleus fraction, 20 min for the cytoplasm fraction for each drying step) followed by addition of urea and sample buffer (20 μ l for the nucleus fraction, 30 μ l for the cytoplasm fraction). The samples were placed in an ultrasonic bath (intensity: 70%, 5 min, 23°C) and protein solutions were obtained by drawing the samples and ejecting them back into the falcon with a pipette. The produced foam was removed by placing the samples at -80°C for 2 min, and centrifugation (1300 rpm, 3 min, 23°C, acceleration 9, deceleration 9). In order to solve the entire pellet of cytoplasm proteins the same process of urea- and sample buffer-adding (10 μ l), followed by sonication, mixing with a pipette and foam removing as described above was performed twice. The obtained protein solutions were transferred in eppendorf tubes. In order to increase the protein yield, the protein residues in the falcons were solved in 10 μ l sample buffer (nucleus fraction) and 20 μ l sample buffer (cytoplasm fraction) according to the process described above. The obtained solutions were added to the corresponding protein solutions in the eppendorf tubes and the samples were stored at -20°C.

2.2.2 Harvesting of cells and preparation of metabolite extracts from whole cell lysates for metabolomics experiments

After incubation (see section 2.1.4), the 6 well plates were removed from the incubator and placed on ice. The cell culture media were removed and 100 μ l of ethanol/phosphate buffer (85/15) were pipetted in each well. The cells were scraped off from the bottom of the wells; the suspensions were homogenized with a pipette and transferred into falcons. In order to increase the yield, another 100 μ l of the ethanol/phosphate buffer were added to each well, followed by a homogenizing step with a pipette. The cell suspensions were transferred in the falcons. Cell disruption was performed by sonication of each suspension followed by centrifugation (10 min, 3500 rpm, 4°C, acceleration 9, deceleration 9). The resulting supernatants were transferred into eppendorf tubes and stored at -80°C.

2.2.3 Bradford assay

All protein concentrations in the samples prepared for shotgun proteomics (preparation described in section 2.2.1) were estimated via Bradford assay. Therefore, the protein solutions, stored at -20°C, were defrosted at room temperature and vortexed. One microliter of each sample was taken and diluted with dest. H₂O (1:200). Furthermore, a solution of Bradford reagent was added to the diluted protein solution (Bradford reagent/protein solution: 1:5), followed by vortexing. A blank solution, containing Bradford reagent/H₂O (1:5) was also prepared. The protein concentrations were then estimated by color comparison with a series of standard protein solutions of a protein concentration range between 0 and 4 µg/µl. In the case of a protein concentration exceeding the concentration range of the standard series (intensity of the blue colour higher in comparison with that of the 4 µg/µl standard), the sample was diluted with a Bradford/water mixture (1:5) to the ratio of 1:2. The dilution step was repeated until the protein concentration of the sample was within the range of the standard series. Thus, after *n* dilution steps the original protein concentration in the sample was calculated as *n*-fold of the diluted protein concentration. The resulting protein concentrations are listed in the tables below.

Table 1. Protein concentrations of the cell fractions from the preliminary test

Cell fraction	Protein concentration [µg/µl]
Cytoplasm	1.25
Nucleus	14

Table 2. Protein concentrations of SKOV3 samples after 8h of incubation (control and with FASN inhibitor incubated groups)

Sample ID	Cell fraction	Protein concentration [µg/µl]
Control 1	nucleus	5.5
	cytoplasm	16.25
Control 2	nucleus	5.5
	cytoplasm	16.25
Control 3	nucleus	2.75
	cytoplasm	8.75
Incubation with FASN inhibitor 1	nucleus	5.5
	cytoplasm	16.25
Incubation with FASN inhibitor 2	nucleus	5.5
	cytoplasm	16.25
Incubation with FASN inhibitor 3	nucleus	2.75
	cytoplasm	16.25

Table 3. Protein concentrations of SKOV3 samples after 24h of incubation (control and with FASN inhibitor incubated groups)

Sample ID	Cell fraction	Protein concentration [µg/µl]
Control 1	nucleus	3
	cytoplasm	13.75
Control 2	nucleus	4.5
	cytoplasm	13.75
Control 3	nucleus	4.5
	cytoplasm	13.75
Incubation with FASN inhibitor 1	nucleus	3
	cytoplasm	13.75
Incubation with FASN inhibitor 2	nucleus	3
	cytoplasm	13.75
Incubation with FASN inhibitor 3	nucleus	3
	cytoplasm	15

2.3 Shotgun proteomics

2.3.1 In-gel digestion

In-gel digestion was performed with protein extracts obtained from SKOV3 cells cultivated in T75 flasks (see section 2.1.2 and 2.2.1) prepared for proteomic characterization of the cells.

2.3.1.1 Preparation of 1D-SDS-acrylamide gel

The slab gel unit with the glass sandwich set (1mm spacer) was cleaned with a water/ethanol solution (10/70), assembled in the casting frame and placed on the casting stand. The front between the stacking gel and the separating gel was marked (2.5 cm away from the top of the short plate). The separating and the stacking gels were prepared as described below (see appendix). One milliliter of the separating gel was used for the production of a cork gel, which was pipetted on the bottom of the glass sandwich and was allowed to fully polymerize. The stacking and separating gel solutions were degassed in a desiccator for 10-15 min and the polymerization reaction in the separating gel solution was induced by addition of the reagents listed in the appendix. The gap between the glass plates was filled with the separating gel mixture until the marked front and, in order to obtain a horizontal gel surface, a 90% isopropanol solution was overlaid. The gel was allowed to completely polymerize for

30 min, after what the isopropanol solution was discarded with filter paper. The stacking gel was then completed by adding SDS, APS and TEMED (see Table 9; appendix) and pipetted on top of the separating gel; the slot-forming comb was inserted without trapping air under the teeth. The stacking gel was allowed to fully polymerize for 1h.

2.3.1.2 Sample loading

Both samples were mixed with H₂O and 5xSDS-PP in the volumes shown in Table 4. Each blank solution was prepared by mixing 24 μ l sample buffer with 6 μ l 5xSDS-PP. The protein marker (5 μ l) was mixed with 6 μ l 5xSDS buffer and 19 μ l H₂O.

The polyacrylamide gel was removed from the casting frame and attached to the electrode assembly together with a plastic plate on the other side. The space between the plates was filled with electrode buffer and the slot-forming comb was removed. Table 4 shows a list of the solutions loaded on each gel position from 1 to 10 (left to right). The following protein amounts were loaded: 80 μ g from the cytoplasm fraction, 20 μ g from the nuclear fraction.

Table 4. 1D-SDS-PAGE: sample loading; CYT: cytoplasmic fraction, NE: nuclear fraction

Gel position	Sample name	Protein concentration [μ g/ μ l]	Loaded sample volume [μ l]	Water volume [μ l]	5xSDS-PP volume [μ l]	Total volume [μ l]
1	Blank	-	-	-	-	30
2	Blank	-	-	-	-	30
3	SKOV3 NE	1.25	16	8	6	30
4	Blank	-	-	-	-	30
5	Blank	-	-	-	-	30
6	SKOV3 CYT	14.0	5.7	18.3	6	30
7	Blank	-	-	-	-	30
8	MW-Maker	-	-	-	-	30
9	Blank	-	-	-	-	30
10	Blank	-	-	-	-	30

2.3.1.3 SDS-gel electrophoresis

The electrode assembly was placed in the tank filled with electrode buffer and the tank lid was placed on top. Gel electrophoresis was performed with the following parameters:

- adjusted current: 20mA
- adjusted voltage: 200V
- duration: until the marker was completely separated, or when the smallest molecules had covered a distance of 1cm in the separating gel which was indicated by the colored marker (bromphenol blue) migrating with the front.

After switching off the apparatus, the electrode assembly was removed and the electrode buffer between the plates was poured back into the tank. The glass sandwich set was removed from the electrode assembly and the glass plates were separated from each other. The polyacrylamide gel was placed in a fixing solution of methanol/acetic acid/water (50/10/40) overnight.

2.3.1.4 Silver staining

All steps of the silver staining were performed under shaking of the gel. The fixing solution was removed and the gel was washed with a solution of methanol/water (1:1) for 10 min. Two more washing steps with bidest. H₂O (5 min each) were performed, followed by a sensitization step with a solution of 0.02% sodium thiosulfate for 1 min. The gel was then briefly washed twice with bidest. H₂O, followed by silver impregnation with a 0.1% AgNO₃ solution for 10 min. The gel was again briefly washed with water and shaken in a 3% Na₂CO₃/0.05% HCHO solution (development) until sufficient staining was achieved (immediately after staining of the protein bands). The developing step was stopped by replacing the solution with a 1% acetic acid solution. After 5 min of shaking, the gel was photographed.

2.3.1.5 In-gel digestion

The gel was put onto a light box and photographed. The protein bands were excised and each band was divided in four parts as shown in Figure 12.

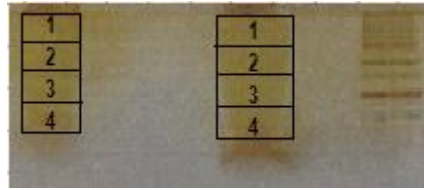


Figure 12. SDS-PAGE of preliminary experiment samples; left: nuclear fraction; middle: cytoplasmic fraction; right: marker

Thus, each cytoplasm band contained approximately 20µg of protein, while each nucleus band contained approximately 5µg of protein. The bands were cut into cubes (ca. 1x1 mm) and transferred into eppendorf tubes. 200µl of destaining solution (15mM $K_3Fe(CN)_6$, 50mM $Na_2S_2O_3$) was added into each eppendorf tube and the samples were shaken (1400 rpm, 25°C) until destaining (colorless gel pieces) was reached. The samples were shortly centrifuged and the destaining solution was discarded, followed by a pH adjusting/washing step. Each protein band was washed four times with alternating 25 mM ammonium bicarbonate buffer (ABC, 2.5ml 500mM ABC + 47.5ml des. H_2O) and acetonitrile (ACN) by the following procedure: 400µl of the washing solution was added, followed by shaking (10min, 1400 rpm, 25°C). The samples were then shortly centrifuged and the solution was removed.

The protein reduction was performed by adding 200µl of a 10mM dithiotreitol solution (50µl 1M DTT + 4.95ml 25mM ABC) to each 5µg-protein band and 200µl of a 20mM DTT solution (100µl 1M DTT + 4.9ml 25mM ABC) to each 20µg-protein band. The samples were then shaken (30 min, 56°C, 1100 rpm), shortly centrifuged and the solution was discarded. The samples were washed once with 25mM ABC buffer and once with acetonitrile according to the procedure described above.

The alkylation step occurred with 50mM iodoacetamide (IAA) (for 5µg protein/band, 250µl 500mM IAA + 4.75ml 25mM ABC) or 100mM IAA (for 20µg protein/band, 500µl 500mM IAA + 4.5ml 25mM ABC). The samples were shaken in 200µl solution for 30 min, at 1200 rpm, 37°C, in the dark and washed four times with alternating 25mM ABC buffer and ACN as already described.

The samples were dried in the speedvac for 15 min at 40°C and placed on ice. Trypsin/LysC aliquots (previously stored at -80°C) were thawed at 4°C and 10µl were diluted 1:16 with ice cold 50mM ABC buffer, and 15µl of the diluted enzyme solution was added to each 5µg protein band (ca. 0.09µg trypsin per protein band). For the 20µg protein bands, 10µl trypsin/LysC aliquots were diluted 1:4 with ice cold 50mM ABC buffer and 20µl of the solutions were pipetted into the samples (0.5µg trypsin/LysC per protein band). After 10 min, 20µl of icecold 50mM ABC buffer was added to each sample in order to cover all gel pieces with the enzyme solution. The samples were incubated overnight at 37°C.

After the overnight incubation with enzymes, a second portion of trypsin/LysC was added to the samples, as described above, followed by incubation at 37°C for 4h. The resulting peptide solutions were vortexed, removed from the gels and pipetted

into siliconised eppendorf tubes. Further peptide extraction from the polyacrylamide gel was performed with 25mM ABC solution (3 x 40µl) and 5% formic acid (2 x 40µl). The pipetted extraction solutions were vortexed, followed by shaking (15 min, 1400 rpm, 37°C), short centrifugation and transferred into the corresponding siliconised eppendorf tube.

The obtained peptide solutions were dried in the speedvac (40°C, until all liquid was vaporized) and stored at -20°C until MS measurement was performed.

2.3.2 In-solution digestion

Protein samples obtained from cell culture experiments undertaken to analyze the effects of FASN inhibitor treatment of SKOV3 cells (see section 2.1.3, 2.1.4 and 2.2.1) were further processed by in-solution digestion. First, samples were defrosted at room temperature and vortexed. For in-solution digestion, 25µg of protein were taken from each sample. The corresponding sample volumes are given in Tables 5 and 6.

Table 5. Sample volumes used for in-solution digestion (8h incubation series); Con: control sample; NE: nucleus fraction; CYT: cytoplasmic fraction

Sample ID	Protein concentration [µg/µl]	Sample volume used [µl]
Con 1 NE	5.5	4.5
Con 2 NE	5.5	4.5
Con 3 NE	2.75	9.1
With FASN inhibitor 1 NE	5.5	4.5
With FASN inhibitor 2 NE	5.5	4.5
With FASN inhibitor 3 NE	3	8.3
Con 1 CYT	16.25	1.5
Con 2 CYT	16.25	1.5
Con 3 CYT	8.75	2.9
With FASN inhibitor 1 CYT	16.25	1.5
With FASN inhibitor 2 CYT	16.25	1.5
With FASN inhibitor 3 CYT	16.25	1.5

Table 6. Sample volumes used for in-solution digestion (24h incubation series); Con: control sample; NE: nuclear fraction; CYT: cytoplasmic fraction

Sample ID	Protein concentration [µg/µl]	Sample volume used [µl]
Con 1 NE	3	8.3
Con 2 NE	4.5	5.6
Con 3 NE	4.5	5.6
With FASN inhibitor 1 NE	3	8.3
With FASN inhibitor 2 NE	3	8.3
With FASN inhibitor 3 NE	3	8.3
Con 1 CYT	13.75	1.8
Con 2 CYT	13.75	1.8
Con 3 CYT	13.75	1.8
With FASN inhibitor 1 CYT	13.75	1.8
With FASN inhibitor 2 CYT	13.75	1.8
With FASN inhibitor 3 CYT	15	1.7

Each protein solution was added to 200µl of a mixture of DTT (5mg/ml) and guanidinium hydrochloride (8M) solved in 50mM ABC buffer (5ml 500mM ABC + 45ml dest. H₂O), followed by shaking (1400 rpm, 56°C, 30min). 3kDa MWCO filters were placed in waste tubes and washed by pipetting 500µl of water and centrifugation (14.000g, 15 min). The reduced protein solutions were pipetted onto the filters and the excess reagent was removed by centrifugation (14.000g, 25 min, max. 20µl left on filters). The flow-through was discarded and the samples were washed by adding 200µl of 50mM ABC buffer and centrifugation (14.000g, 25 min, max. 20µl left on filters). 200µl of a mixture of IAA (10mg/ml) and guanidinium hydrochloride (8M) in 50mM ABC buffer were added onto each filter, the solutions were mixed and shaken (45 min, 30°C, 1000rpm, in the dark). The excess reagent was removed with another centrifugation step (14.000g, 25min, 5µl or less left on filter) and the samples were washed with 200µl of a 50mM ABC buffer as described above (max. 5µl left on filter). The filters were then placed in sterile tubes and on ice together with the trypsin stock solutions. 0.5µg trypsin/LysC solved in 100µl ice cold 50mM ABC buffer was added to each filter, followed by mixing with a pipette, shaking (5°C, 1000rpm, 10min) and incubation (37°C, overnight).

The filters were placed on ice again and a second portion of trypsin/LysC (0.5µg solved in 50µl ice cold 50mM ABC buffer) was added. The samples were mixed well with a pipette and incubated again (37°C, 4h). The resulting peptide solutions were centrifuged (20min, 14.000g, until all liquid is through), 40µl 50mM ABC buffer was pipetted on each filter and it was centrifuged again (15 min, 14.000g). The filters were

removed and the peptide solutions were acidified with 10% trifluoroacetic acid (TFA) to the final concentration of 1% TFA.

Before sample loading, the C18 spin columns were placed in 2ml eppendorf tubes and washed twice by pipetting 500µl 50% ACN and centrifuging for 1min at 1500g. The columns were equilibrated by loading 200µl of a 5% ACN/ 0.5% TFA solution and centrifugation for 1min at 1500g. This procedure was performed twice. The samples were then pipetted onto the columns and centrifuged (1min, 1500g). The flow-through was reloaded onto the columns and again centrifuged (1min, 1500g). The flow-through was discarded, followed by a washing step: centrifugation of 200µl 5% ACN/ 0.5% TFA solution through each column (1min, 1500g). The washing step was repeated. The columns were placed into sterile 1.5ml eppendorf tubes and the peptides were eluted twice, each time with 40µl of a 50% ACN/ 0.1% TFA solution, followed by centrifugation (1min, 1500g). The samples were dried in a speedvac (40°C, until all liquid is evaporated) and stored at -20°C until MS measurement was performed.

2.3.3 Mass spectrometry measurement

Each sample prepared for shotgun analysis (see sections 2.3.1 and 2.3.2) was first mixed with 5µl of a standard peptide mixture (four standard peptides with the concentration of 10fmol/µl each). The samples were briefly centrifuged; 40µl of a 98%H₂O/ 2%ACN/ 0.1%FA solution was added and mixed with a pipette. A washing solution was prepared by mixing ACN, FA and the 98%H₂O/ 2%ACN/ 0.1%FA solution in the ratio of 50:15:35. The samples and the washing solution were pipetted on a well plate, which was inserted in the nano-HPLC system UltiMate 3000 RSLC nano Systems (Dionex) in which the produced peptides were separated prior to mass analysis. This system consists of a pre-column (Dionex, Acclaim PepMap 100, C18, 100µm x 2cm) and a separating column (Dionex, Acclaim PepMap RSLC, C18, 75µm x 50cm). Loading of the sample to the pre-column was achieved using a flow rate of 10µl/min. The peptide elution was achieved by nano-flow, using a linear gradient within 40min, starting with 99% solvent A and 1% solvent B and ending with 60% solvent A and 40% solvent B. The nano-flow rate was adjusted to 300nl/min, the pressure was 550bar with a temperature of 40°C. The composition of solvent A was 98% H₂O, 2% ACN and 0,1% FA, whereas the composition of solvent B was 80% ACN, 20% H₂O und 0,1% FA. The sample volume for each analysis was 5µl. After each set of eight LC-MS runs, a washing step as well as a quality control containing the standard peptide mixture were run. Peptide identification was performed with a QExactive mass spectrometer (Thermo Fisher Scientific), where species within the peptide mass range (400-1400 m/z) were selected in the quadrupole. MS/MS spectra were obtained by fragmentation of the six most abundant precursor ions from the MS scan, which were isolated and fragmented via higher-energy collisional induced dissociation (HCD) using nitrogen gas. Each sample was measured twice (technical duplicates).

2.3.4 Data analysis

2.3.4.1 Proteome discoverer

The obtained ms-data were analyzed via “Proteome discoverer 1.4” (Thermo Fisher Scientific). Proteome discoverer may use several search engines such as SEQUEST and Mascot to identify peptide sequences from the mass spectra of digested peptides. Protein identification results from a search in the Uniprot database (human). Here, Mascot was used and the following search parameters were adjusted:

- Maximal missed cleavages: 2
- Peptide tolerance: ± 5 ppm
- MS/MS tolerance: ± 20 ppm
- Fixed modification: Carbamidomethylation (C)
- Variable modification: Oxidation (M), Acetylation (N-term.)
- False discovery rate (FDR): 0.01
- Mascot score significance threshold: 0.05

2.3.4.2 Max Quant search

The analysis of the data obtained from the experiments undertaken to determine the effects of the FASN inhibitor treatment on SKOV3 cells was supported by label-free quantification via the open source software MaxQuant [27]. The Max Quant search was performed by loading the respective raw files (txt.files) and adjusting the following parameters:

- Variable modification: Oxidation (M), Acetylation (N-term.)
- Fixed modification: Carbamidomethylation (C)
- Multiplicity: 1
- First search: 50ppm
- Main search: 25ppm
- Modifications per peptide: 2
- Maximal missed cleavages: 2
- Maximal charge: 5
- Database used: Uniprot_Human
- Peptide FDR: 0.01
- Site FDR: 0.01
- Maximal peptide PEP: 1
- Minimal peptides per protein: 2
- Minimal unique peptides per protein: 1
- Protein FDR: 0.01
- Label-free quantification

2.3.4.3 Max Quant data processing

The data obtained from the Max Quant search were processed with the aid of the Perseus statistical analysis package included in the MaxQuant software [27]. After data loading, significant peptides were selected by removing all non-relevant proteins (only identified by site, reverse sequences and contaminants). The logarithms (base 2) of all protein quantity values were calculated and sample groups were formed. All biological and technical replicates of a single cellular state (same incubation time, incubation medium (with FASN-inhibitor or with pure DMSO) and cellular fraction) were placed in one protein group. Subsequently, the valid values within a protein group were filtered (minimal number of valid values within at least one group: 4). For relative quantification, missing quantitative values were replaced by an imputed value derived from a normal distribution (width 0.3; down shift: 1.8). Differences in protein abundances between control cells and with FASN-inhibitor treated cells (same incubation times and cellular fractions) were determined. Significant differences were assessed using a t-test. Subsequently, fold change values were calculated from the obtained t-values according to the following formula: Fold change = $\log_2(\text{t-value})$. For data analysis, the proteins with a p-value lower than 0.05 and fold change of ≥ 1 or ≤ -1 were used.

2.4 Targeted metabolomics

In a targeted metabolomics assay, the following metabolite groups were analyzed: amino acids, biogenic amines, acylcarnitines, glycerophospholipids, sphingolipids and hexose. This was done by using the AbsoluteIDQ™ p180 Kit, which is able to quantify up to 188 of species of the above mentioned metabolic groups. The method combines sample preparation (extraction and derivatisation of the analytes) and a selective mass spectrometry detection using MRM pairs. Analyte quantification was achieved using isotope-labeled internal standards and other internal standards. The Kit is suitable for FIA-MS/MS and LC-MS/MS assays. Biocrates proprietary MetIDQ™ software allows automation of the assay workflow from sample registration to data processing. [33]

2.4.1 Preparation of reagents and solvents

The metabolome samples (preparation described in section 2.2.2) were stored at -80°C together with the Biocrates Kit plate (under nitrogen gas), all internal standards, calibration standards, the derivatisation reagent (Phenylisothiocyanate (PTIC)) and quality control samples. All samples, materials and reagents were defrosted at room temperature and the sample volumes were estimated using a pipette. It was observed that ethanol had partially evaporated during cell disruption (sample volume decrease in comparison to the solvent volume used for cell disruption (200µl), see Table 7).

Table 7. Metabolomics assay: sample volumes, con: control sample

Sample ID	Sample volume [μ l]
Con 1; 8h	90
Con 2; 8h	120
Con 3; 8h	100
With FASN inhibitor 1; 8h	0
With FASN inhibitor 2; 8h	110
With FASN inhibitor 3; 8h	95
Con 1; 24h	95
Con 2; 24h	100
Con 3; 24h	115
With FASN inhibitor 1; 24h	110
With FASN inhibitor 2; 24h	115
With FASN inhibitor 3; 24h	110

All needed solutions were prepared as described:

- Internal standard (ISTD) mixture for LC-MS method: 1200 μ l of HPLC grade water were added to the lyophilized ISTD mixture and a solution was obtained by shaking (15min, 1200rpm) and multiple vortexing. The ISTD for the FIA method are implemented in the Kit plate.
- Quality control (QC) solutions: 100 μ l of HPLC grade water were added to each QC sample, followed by shaking (15min, 1200rpm) and multiple vortexing until clear solutions were obtained. Before loading onto the Kit plate, the QC solutions were centrifuged for 5min at 2750g and 4°C.
- Calibration standards: 100 μ l of HPLC grade water were added to each of the seven calibration standards. They were shaken (15min, 1200rpm) and vortexed. Before loading the standard solutions onto the Kit plate, the tubes were gently taped on order to collect the solutions on the bottom of the tubes.
- Pre-mix for derivatisation: The pre-mix was prepared by mixing ethanol, water and pyridine (1:1:1) to the final volume of 5700 μ l.
- Phenylisothiocyanate (PITC) derivatisation solution: 300 μ l of PITC were added to the premix, the mixture was vortexed until a clear solution was obtained (5% v/v PITC). Since the stability was reduced after adding PITC to the premix, this solution was prepared immediately before derivatisation.
- Extraction solvent: A 50mM ammonium acetate solution was prepared by solving 19mg of ammonium acetate in 50ml grade HPLC methanol.
- Blank solution: 7.5ml phosphate buffer (preparation see appendix) were mixed with ethanol (-20°C) to the final volume of 50ml (phosphate buffer/ethanol: 15:85)
- FIA running solvent: The content of a FIA running solvent ampule was diluted with 290 μ l HPLC grade methanol.

2.4.2 Preparation of the Biocrates p180 Kit plate

The plastic lid was removed from the Kit plate and 10µl of the internal standard mix (ISTD) were pipetted to each well, except for the blank well position. 10µl of each calibration standard, quality control sample and blank solution and 20µl of the samples were pipetted on the center of the wells. Each sample was pipetted in duplicates on the plate. The solutions were dried under nitrogen flow (3-4 bars, 20min), followed by a second sample application (20µl) and drying under the same conditions. 50µl of the freshly prepared PITC solution was added to the wells and the plate was covered with the plastic lid. The derivatisation reaction took place at room temperature for 20min. The plastic lid was removed and the plate was dried under nitrogen gas for 60 min. 300µl of extraction solvent was added to each well and the plate was covered with the plastic lid again. The plate was shaken at 450rpm and room temperature for 30min, followed by centrifugation (5min, 500g, room temperature). The lower capture plate containing the analyte extracts was separated from the upper filter plate. 140µl from each extract were transferred into an empty 96-well plate and 140µl of HPLC grade water was added. The silicon mat was placed onto the plate, which was shaken for 2min at 600rpm. This plate was further used for LC-MS measurement, while the rest of extraction solvent was used for flow injection analysis (FIA). 400µl of the FIA running solvent were added to each well of the FIA-plate, the plastic lid was put onto the plate and it was shaken for 2min at 600rpm. The samples were measured immediately.

2.4.3 Biocrates p180 Kit measurement

All amino acids and biogenic amines were detected via LC-MS/MS, while for the phospholipids, acylcarnitines and hexose FIA-MS/MS was used. As the calibration standard mix (preparation see section 2.4.1) did not contain glycerophospholipids and sphingolipids, these species could be analysed only in a semi quantitative manner by comparison of the analyte signal and the signal of the corresponding internal standard. A more accurate quantitation of all other analytes was possible with the aid of calibration functions of the corresponding calibration standards.

The prepared plate was placed in the autosampler at 10°C. After each injection, a needle wash step was integrated in order to avoid cross contaminations (wash solvent for the LC-MS/MS assay: water; wash solvent for the FIA-MS/MS assay: 33% methanol, 33% isopropanol, 33% water). During LC-MS/MS, a separation of the analytes was performed with an Agilent 1290 Infinity UHPLC system, which consists of a pre-column and a separating column (C18). The FIA-MS/MS analysis was performed with an Agilent 1200 Rapid resolution device. The multiple reaction monitoring (MRM) analysis was performed with an AB Sciex 4000 QTrap mass spectrometer, coupled with an ESI ionisation source.

The injection volume for the LC-MS/MS method was 5µl and the flow rate was 900µl/min. The analyte elution was performed by using a linear gradient within 6

minutes starting with 100% solvent A and ending with 100% solvent B. The composition of solvent A was 0.2% formic acid in HPLC grade water, while the composition of solvent B was 0.2% formic acid in acetonitrile. Before starting the assay, the pre-column was purged with 100% solvent B with a flow rate of 1ml/min for 5min. The pre-column and the column were connected and the system was washed with 100% solvent B at a flow rate of 900 μ l/min for 15min (stepwise increase of the flow rate), followed by an equilibration step with 100% solvent A for 10min.

For the FIA assay, the UHPLC column was removed and the autosampler was directly connected with the MS ion source. The injection volume was set to 20 μ l.

2.4.4 Data analysis

For each cellular state (control cells, 8h and 24h; with FASN-inhibitor treated cells, 8h and 24h), biological triplicates and technical duplicates were produced, resulting in six measurements for each metabolite, respectively. Comparison of metabolite concentrations between control cells and treated cells of the same incubation time was made. At first, an F-test with the concentration values of each metabolite between the groups was made. This test compares the concentration variances between two groups and allows us to assess whether the variance differences are significant. Furthermore, depending on the obtained results from the F-test, the appropriate t-test was performed. In other words, if there was significant difference between the variances of two groups, a t-test assuming unequal variances was applied. For the rest of the data, a t-test assuming equal variances was used. Finally, concentration means for each analyte and each group were calculated and the concentration differences between two groups were estimated by the following formula:

Concentration difference = concentration mean (in cells treated with FASN) [μ M] – concentration mean (control cells) [μ M]

This implies that a negative value corresponds to the down-regulation, while a positive value corresponds to the upregulation of a given metabolite.

3 Results

3.1 Cell culture experiment

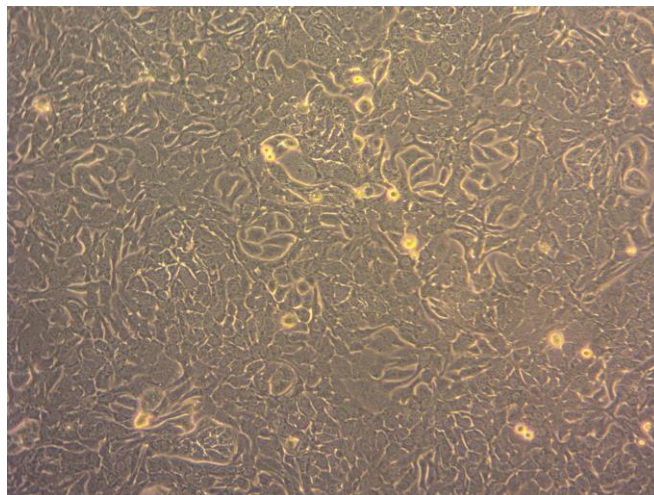
Figure 13 shows pictures of the SKOV3 cells before and during the experiments. All cells show confluence; the viability of the cells used for cell characterization was 0.94, while the viability of the cells used for the experiment with the FASN inhibitor was 0.91.

Cell number (cell characterization): $3.16 \cdot 10^6$

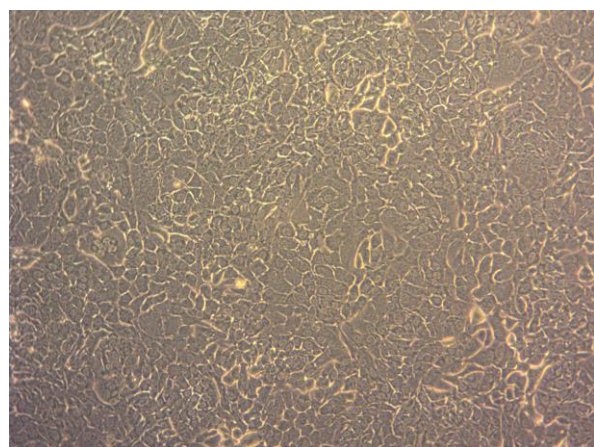
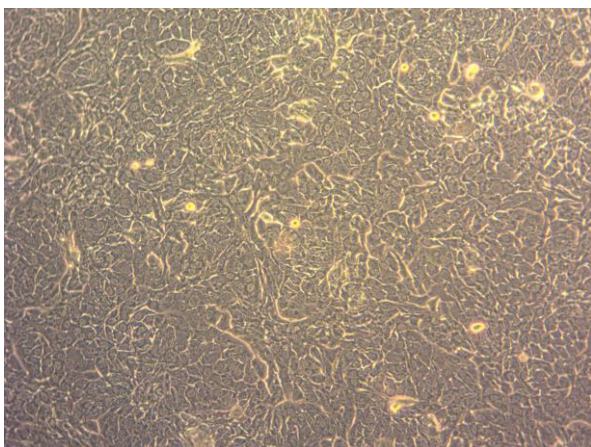
Cell number (T25 flasks): between $1 \cdot 10^6$ and $2 \cdot 10^6$ per flask

Cell number (6 well plates): between $0.5 \cdot 10^6$ and $1 \cdot 10^6$ per well plate

a)



b)



c)

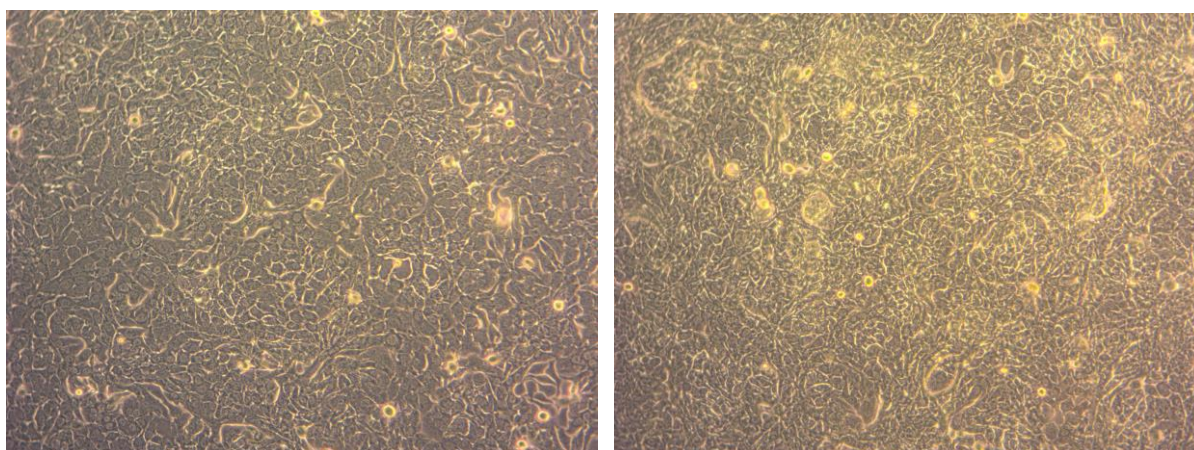


Figure 13. Cell cultures; a) before cell characterization; b) cells after 8h of incubation: control (left) and with FASN inhibitor (right); c) cells after 24h of incubation: control (left) and with FASN inhibitor (right)

3.2 Proteome profiling

3.2.1 SKOV3 cell characterization

Table 8 shows a list of proteins obtained after proteome profiling of non-treated SKOV3 cells. The results, presented below, suggest that *de novo* fatty acid synthesis takes place in this ovarian cancer cell line since the fatty acid synthase was identified with high confidence (score: 31869; coverage: 60%, unique peptides: 101) in these cells. Moreover, other proteins involved in the FASN up-regulation, as previously described (see section 1.3.2), were also detected. Such proteins were, for example, ErbB-2, EGFR, AKT and MAPK, which stimulate cell growth and therefore also activate FASN transcription. The transcription factor FBI-1, which boosts FASN expression, was also detected in the nuclear fraction of the cells. Obviously, cell growth signaling pathways were activated in the ovarian cancer cell line, resulting in FASN over-expression. It should therefore be assumed that the ovarian cancer cell line SKOV3 is sensitive against FASN-blockers.

Table 8. Proteins present in the SKOV3 ovarian cancer cell line (preliminary experiment)

Protein name	Subcellular location	Score	Coverage	Unique peptides	Peptides
Fatty acid synthase (FASN)	cytoplasm	31869	60%	101	101
Receptor tyrosine-protein kinase ErbB-2	cytoplasm	10630	54%	39	43
Epidermal growth factor receptor (EGFR)	cytoplasm	3407	32%	26	28
Mitogen-activated protein kinase 1 (MAPK1)	cytoplasm	3555	75%	16	21
RAC-alpha serine/threonine-protein kinase (AKT1)	cytoplasm	678	32%	9	11
Zinc finger and BTB domain-containing protein (FBI-1)	nucleus	405	25%	1	7
Serine/threonine-protein kinase (mTOR)	cytoplasm	771	11%	17	17

3.2.2 Proteome profiling after FASN-inhibition

3.2.2.1 Down-regulated proteins

After incubation with the FASN inhibitor, a large number of proteins involved in cell cycle progression were found to be down-regulated in SKOV3 cells (Table 9). These proteins had functionalities in different processes related to cell cycle progression such as mitotic spindle formation (e.g. tubulin beta chain, centrosomal protein of 78kDa, mitotic spindle organizing protein), chromosome segregation and condensation (e.g. mitotic spindle-associated MMXD complex subunit MIP18, regulator of chromosome condensation), cytokinesis (e.g. Rac GTPase-activating protein 1), or fragmentation of Golgi stacks during mitosis and their reassembly after mitosis (e.g. transitional endoplasmic reticulum ATPase). Others were important for the transition of one mitotic phase to another, such as cyclin-dependent kinase 1, known to promote the G2-M and the G1-S transition, or for important functions

throughout the mitotic phase, such as the serine/threonine protein kinase PLK1, which is active during the M-phase. Interestingly, for this protein the down-regulation was more pronounced after 24 hours (3.30 fold) than after 8 hours (0.66 fold), suggesting an increase of the cytostatic effect of the FASN blocker with time.

Table 9. Down-regulation of proteins related to cell cycle progression, induced by FASN inhibition; CYT: cytoplasmic fraction; NE: nuclear fraction; fold change relative to controls in a logarithmic scale to the base 2; “-”, the protein was not detected in the respective samples.

Protein name	8h				24h			
	CYT		NE		CYT		NE	
	p value	fold change	p value	fold change	p value	fold change	p value	fold change
Tubulin beta chain	-	-	-	-	8,59E-04	-1,08	-	-
Centrosoma I protein of 78 kDa	-	-	-	-	3,00E-04	-1,14	-	-
Mitotic spindle-associated MMXD complex subunit MIP18	-	-	-	-	3,22E-02	-1,15	-	-
Cyclin-dependent kinase 1	-	-	-	-	4,68E-03	-1,37	1,02E-03	-1,93
Transforming acidic coiled-coil-containing protein 3	-	-	-	-	1,01E-05	-1,85	-	-
Tubulin beta-4A chain	4,84E-02	1,87	-	-	2,87E-03	-1,93	-	-
G2/mitotic-specific cyclin-B1	3,53E-02	-1,26	-	-	2,19E-04	-2,29	1,03E-2	-0,73
Kinesin-like protein KIF23	-	-	-	-	1,63E-04	-3,05	3,52E-02	-1,22
Serine/threonine-protein kinase PLK1	2,27E-02	-0,66	-	-	1,64E-04	-3,30	3,33E-03	-2,20
Leucine-rich repeat and WD repeat-containing protein 1	1,18E-02	-1,01	-	-	-	-	-	-
1-phosphatidylinositol	4,73E-03	-1,01	-	-	-	-	-	-

4,5-bisphosphate phosphodiesterase delta-3								
Mitotic-spindle organizing protein 2A,2B	3,13E-02	-1,05	-	-	-	-	-	-
Nucleoporin Nup43	1,46E-02	-1,15	-	-	3,12E-02	-0,62	1,46E-02	-1,23
DNA replication licensing factor MCM4	1,88E-02	-1,19	9,69E-03	0,82	-	-	3,44E-02	0,48
Fizzy-related protein homolog	3,96E-03	-1,20	-		-	-	-	-
Cell division cycle protein 123 homolog	2,88E-02	-1,21	-	-	-	-	-	-
Regulator of chromosome condensation	3,82E-04	-1,30	-	-	-	-	-	-
Septin-8	2,45E-02	-1,49	-	-	-	-	-	-
Transforming acidic coiled-coil-containing protein 1	2,85E-04	-1,59	7,77E-03	-0,66	-	-	-	-
Regulator of microtubule dynamics protein 1	4,59E-02	-1,72	-	-	-	-	-	-
Protein S100-A7	1,11E-02	-2,26	-	-	-	-	-	-
Protein ECT2	-	-	-	-	-	-	3,10E-02	-1,14
CCR4-NOT transcription complex subunit 3	-	-	4,51E-02	0,79	-	-	1,55E-02	-1,16
Serine/threonine-protein phosphatase PP1-gamma catalytic subunit	-	-	-	-	-	-	4,13E-02	-1,27

TFIIH basal transcription factor complex helicase XPD subunit	-	-	-	-	-	-	3,01E-02	-1,31
Nucleoporin SEH1	-	-	-	-	-	-	1,43E-02	-1,34
Kinesin-like protein KIF22	-	-	-	-	-	-	2,26E-02	-1,40
Protein NEDD1	-	-	-	-	-	-	2,82E-02	-1,41
ADP-ribosylation factor-like protein 2	-	-	-	-	8,21E-03	-0,74	1,18E-02	-1,68
Cell division cycle-associated protein 2	-	-	-	-	-	-	2,24E-02	-1,79
Ras association domain-containing protein 7	-	-	-	-	-	-	1,56E-02	-1,98
MAU2 chromatid cohesion factor homolog	-	-	-	-	-	-	1,70E-02	-1,98
Serine/threonine-protein phosphatase 4 catalytic subunit	-	-	-	-	-	-	9,73E-03	-2,26
Small kinetochore-associated protein	-	-	-	-	-	-	4,66E-04	-2,53
Inner nuclear membrane protein Man1	-	-	-	-	-	-	7,39E-03	-2,75
Transitional endoplasmic reticulum ATPase	-	-	2,32E-03	-1,03	-	-	1,77E-02	-0,62
Protein pelota homolog	-	-	1,64E-02	-1,04	-	-	1,08E-02	0,71
Nuclear protein localization protein 4 homolog	-	-	4,84E-04	-1,04	3,48E-02	-0,23	-	-

tRNA (cytosine(34)-C(5))- methyltrans ferase	-	-	4,11E-03	-1,09	-	-	-	-
Ubiquitin- conjugating enzyme E2 N	-	-	2,72E-02	-1,10	-	-	-	-
NSFL1 cofactor p47	-	-	5,04E-03	-1,53	1,71E-03	-0,48	-	-
Nuclear migration protein nudC	-	-	2,89E-02	-1,76	2,36E-03	-0,56	-	-
NEDD8- activating enzyme E1 catalytic subunit	-	-	3,83E-02	-1,89	-	-	-	-
Protein VPRBP	-	-	-	-	-	-	1,76E-02	-1,29
Proline-, glutamic acid- and leucine-rich protein 1	-	-	-	-	-	-	4,54E-02	-1,32
Histone lysine demethylas e PHF8	-	-	7,85E-03	-1,12	-	-	-	-
Mitogen- activated protein kinase 14	-	-	-	-	-	-	1,76E-02	-1,19
Histone deacetylase 3	-	-	-	-	-	-	1,29E-02	-2,54
Rac GTPase- activating protein 1	-	-	-	-	-	-	2,43E-04	-1,14

Down-regulation of proteins involved in cell growth inducing signaling provided further evidence for the cytostatic effects of the FASN inhibitor. Table 10 shows all down-regulated members of cell growth inducing cascades determined by us, such as coiled-coil domain-containing protein 50 (involved in epidermal growth factor receptor (EGFR) signaling) or serine/threonine-protein kinase mTOR involved in the mTOR signaling, whose oncogenic activation induces several processes required for cancer cell growth, survival and proliferation. [34] Interestingly, the synthesis of nucleotides seemed also to be affected. So, inosine-5-monophosphate dehydrogenase 1, an enzyme involved in synthesis of guanine nucleotides and thus playing an important

role in the regulation of cell growth was found to be down-regulated. In addition, proline-, glutamic acid- and leucine-rich protein 1 was also down-regulated, indicating repression of cell growth and proliferation signaling induced by estrogen.

Table 10. Down-regulation of proteins involved in cell growth, CYT: cytoplasmic fraction; NE: nuclear fraction; fold change relative to controls in a logarithmic scale to the base 2; “-”, the protein was not detected in the respective samples.

Protein name	8h				24h			
	CYT		NE		CYT		NE	
	p value	fold change	p value	fold change	p value	fold change	p value	fold change
Coiled-coil domain-containing protein 50	-	-	-	-	3,78E-02	-1,18	-	-
Growth/differentiation factor 15	-	-	-	-	6,43E-05	-1,44	8,17E-04	-1,36
Serine/threonine-protein kinase mTOR	-	-	-	-	2,40E-02	-1,56	-	-
SHC-transforming protein 1	1,87E-02	-1,41	-	-	-	-	-	-
Inosine-5-monophosphate dehydrogenase 1	4,83E-02	-1,74	-	-	-	-	-	-
Proline-, glutamic acid- and leucine-rich protein 1	-	-	-	-	-	-	4,54E-02	-1,32
Putative hydrolase RBBP9	-	-	-	-	-	-	1,74E-02	-2,19
Hepatoma-derived growth factor-related protein 2	-	-	3,23E-03	-1,07	-	-	2,98E-02	1,47
Growth factor receptor-bound	-	-	1,45E-02	-2,03	1,87E-03	-0,53	7,26E-03	2,08

protein 2								
Inosine-5-monophosphate dehydrogenase 2	-	-	5,72E-03	-2,16	1,34E-02	-0,63	-	-

Impaired fatty acid synthesis was also observed: acetyl-CoA carboxylase 2, an enzyme involved in this process was found to be down-regulated, as well as NADH-cytochrome b5 reductase, required for desaturation and elongation of fatty acids and for cholesterol biosynthesis (see Table 11).

Table 11 Down-regulation of lipid biosynthesis; CYT: cytoplasmic fraction; NE: nuclear fraction; fold change relative to controls in a logarithmic scale to the base 2; “-“, the protein was not detected in the respective samples.

Protein name	8h				24h			
	CYT		NE		CYT		NE	
	p value	fold change	p value	fold change	p value	fold change	p value	fold change
NADH-cytochrome b5 reductase 3	-	-	-	-	2,30E-02	-1,33	-	-
Acetyl-CoA carboxylase 2; Biotin carboxylase	2,70E-03	-3,49	-	-	-	-	2,02E-02	1,35

The energy supply via β -oxidation was also affected by FASN inhibition. Indeed, a decrease of the amount of proteins involved in this process was observed (Table 12.) This is not unexpected, since the β -oxidation uses phospholipids for energy production. [6]

Table 12. Down-regulated proteins involved in β -oxidation, CYT: cytoplasmic fraction; NE: nuclear fraction; fold change relative to controls in a logarithmic scale to the base 2; “-”, the protein was not detected in the respective samples.

Protein name	8h				24h			
	CYT		NE		CYT		NE	
	p value	fold change	p value	fold change	p value	fold change	p value	fold change
Hydroxyacyl-coenzyme A dehydrogenase	-	-	-	-	2,63E-02	-1,46	-	-
Enoyl-CoA hydratase domain-containing protein 3	-	-	-	-	7,55E-05	-2,97	-	-

Importantly, several oncogenic signaling pathways, such as the MAPK, the NF κ B and the Ras pathway, were found to be affected by the FASN blockade as well (Tables 13-15). The MAPK and Ras signaling cascades regulate cell proliferation, survival, growth and migration [35, 36], while NF κ B promotes immunity, inflammation and cell survival.

Table 13. Down-regulated proteins involved in MAPK signaling, CYT: cytoplasmic fraction; NE: nuclear fraction; fold change relative to controls in a logarithmic scale to the base 2; “-”, the protein was not detected in the respective samples.

Protein name	8h				24h			
	CYT		NE		CYT		NE	
	p value	fold change	p value	fold change	p value	fold change	p value	fold change
Ras association domain-containing protein 7	-	-	-	-	-	-	1,56E-02	-1,98
Beta-arrestin-1	-	-	1,79E-03	-1,30	-	-	-	-
Serine/threonine-protein phosphatase 5	1,73E-02	-0,64	3,11E-02	-2,77	-	-	-	-
Ras-related C3 botulinum toxin substrate 1,2,3	-	-	-	-	2,53E-02	-1,11	-	-

Mitogen-activated protein kinase 14	-	-		-	-	-	1,76E-02	-1,19
Transcription factor p65	-	-	4,22E-02	-2,72	-	-	-	-
Mitogen-activated protein kinase 3	-	-	4,46E-02	-1,12	-	-	2,87E-02	1,17
Mitogen-activated protein kinase 1	-	-	4,46E-03	-1,20	6,79E-03	-0,50	-	-
Mitogen-activated protein kinase 14	-	-	-	-	-	-	1,76E-02	-1,19

Table 14. Down-regulated proteins involved in NFκB signaling, CYT: cytoplasmic fraction; NE: nuclear fraction; fold change relative to controls in a logarithmic scale to the base 2; “-”, the protein was not detected in the respective samples.

Protein name	8h				24h			
	CYT		NE		CYT		NE	
	p value	fold change	p value	fold change	p value	fold change	p value	fold change
Transcription factor p65	-	-	4,22E-02	-2,72	-	-	-	-
Mitogen-activated protein kinase 14	-	-	-	-	-	-	1,76E-02	-1,19
Mitogen-activated protein kinase 14	-	-	-	-	-	-	1,76E-02	-1,19

Table 15. Down-regulated proteins involved in Ras signaling, CYT: cytoplasmic fraction; NE: nuclear fraction; fold change relative to controls in a logarithmic scale to the base 2; “-”, the protein was not detected in the respective samples.

Protein name	8h				24h			
	CYT		NE		CYT		NE	
	p value	fold change	p value	fold change	p value	fold change	p value	fold change
Ras-related C3	-	-	-	-	2,53E-02	-1,11	-	-

botulinum toxin substrate 1,2,3								
Transcription factor p65	-	-	4,22E-02	-2,72	-	-	-	-
Mitogen-activated protein kinase 1	-	-	4,46E-03	-1,20	6,79E-03	-0,50	-	-

Other proteins found to be down-regulated upon FASN inhibition were mitochondrial membrane proteins (Table 16) and one protein required for normal function of the Golgi apparatus (Table 17).

Table 16. Down-regulated mitochondrial membrane proteins, CYT: cytoplasmic fraction; NE: nuclear fraction; fold change relative to controls in a logarithmic scale to the base 2; “-”, the protein was not detected in the respective samples.

Protein name	8h				24h			
	CYT		NE		CYT		NE	
	p value	fold change	p value	fold change	p value	fold change	p value	fold change
NADH dehydrogenase [ubiquinone] flavoprotein 2, mitochondrial	-	-	-	-	3,14E-03	-1,06	-	-
Succinate dehydrogenase [ubiquinone] iron-sulfur subunit, mitochondrial	3,25E-04	-1,08	-	-	3,25E-04	-2,02	-	-
Electron transfer flavoprotein-ubiquinone oxidoreductase, mitochondrial	4,10E-02	-1,50	-	-	1,63E-02	-0,78	-	-
Cytochrome b5 type B	1,20E-03	-1,16		-	3,84E-04	-1,24		-

Table 17. Down-regulated protein of the Golgy apparatus, CYT: cytoplasmic fraction; NE: nuclear fraction; fold change relative to controls in a logarithmic scale to the base 2; “-“, the protein was not detected in the respective samples.

Protein name	8h				24h			
	CYT		NE		CYT		NE	
	p value	fold change	p value	fold change	p value	fold change	p value	fold change
Conserved oligomeric Golgi complex subunit 1	-	-	-	-	3,03E-02	-1,35	-	-

Proteins involved in various metabolic processes were also down-regulated in the ovarian cancer cell line upon FASN inhibition (Table 18). These processes were transport of neutral amino acids into the cytoplasm (neutral amino acid transporter B(0)), synthesis of cysteine (1,2-dihydroxy-3-keto-5-methylthiopentene dioxygenase) and synthesis of tyrosin (sepiapterin reductase). Moreover, an increase of the cellular oxidative stress may have occurred, since superoxide dismutase [Cu-Zn], whose role is to neutralize radicals, [33] was also down-regulated.

Table 18. Down-regulation of proteins involved in several metabolic processes, CYT: cytoplasmic fraction; NE: nuclear fraction; fold change relative to controls in a logarithmic scale to the base 2; “-“, the protein was not detected in the respective samples.

Protein name	8h				24h			
	CYT		NE		CYT		NE	
	p value	fold change	p value	fold change	p value	fold change	p value	fold change
Superoxide dismutase [Cu-Zn]	-	-	5,90E-03	-0,75	1,39E-02	-1,06	-	-
Sepiapterin reductase	-	-	-	-	9,00E-03	-1,79	-	-
1,2-dihydroxy-3-keto-5-methylthiopentene dioxygenase	9,52E-03	-0,85	-	-	2,05E-02	-1,95	-	-
Neutral amino acid transporter B(0)	2,68E-02	-1,19	-	-	-	-	-	-

3.2.2.2 Up-regulated proteins

Upregulation of proteins inhibiting cell cycle progression (Table 19) corroborates the theory that treatment with the FASN inhibiting drug causes cell cycle blockade. This blockade appears in the up-regulation of serine/threonine-protein kinase N1 which is involved in the disruption of the tubulin assembly [37] or of transcriptional repressors of genes required for cell cycle progression such as zinc fingers and homeoboxes protein 2, a protein known to repress the promoter activity of the CDC25C gene [38], whose expression is required for activating G2 cells into prophase [39]. Furthermore, up-regulation of Rap1 GTPase-activating protein 1 was observed, which may lead to the inhibition of the mitogenic function of the Ras protein [40], as well as up-regulation of DNA damage checkpoint protein 1, which may induce checkpoint mediated cell cycle arrest.

Table 19. Up-regulated proteins involved in cell cycle arrest, CYT: cytoplasmic fraction; NE: nuclear fraction; fold change relative to controls in a logarithmic scale to the base 2; “-”, the protein was not detected in the respective samples.

Protein name	8h				24h			
	CYT		NE		CYT		NE	
	p value	fold change	p value	fold change	p value	fold change	p value	fold change
Serine/threonine-protein kinase N1	-	-	-	-	-	-	4,05E-03	2,69
Zinc fingers and homeoboxes protein 2	-	-	-	-	-	-	5,38E-04	2,39
CXXC-type zinc finger protein 5	-	-	-	-	-	-	4,51E-03	2,37
Rap1 GTPase-activating protein 1	-	-	-	-	-	-	7,74E-03	2,28
Growth factor receptor-bound protein 2	-	-	1,45E-02	-2,03	-	-	7,26E-03	2,08
Merlin	-	-	-	-	-	-	2,16E-02	1,45
Mediator of DNA damage checkpoint protein 1	-	-	2,94E-02	1,10	-	-	2,98E-04	0,70

Importantly, a clear apoptotic effect was observed after incubation with the FASN inhibitor, as a large number of proteins involved in programmed cell death or proteins contributing to apoptosis were found to be up-regulated (Table 20). One of those was, for instance, THO complex subunit 1, a protein activating caspase-6 [41]. Caspase-6 in turn can activate caspase-8 and lead to the release of cytochrome c from the mitochondrion, which is an essential component of the intrinsic apoptotic pathway [42]. In addition, the up-regulated protein serine protease HTRA2 (mitochondrial) can promote or induce cell death by blockade of the inhibitor of apoptosis proteins (IAPs) [43] involved in cell survival [44]. CXXC-type zinc finger protein 5 is known to activate p53, which in turn can activate the transcription of genes that encode proteins that also promote the release of cytochrome c from mitochondria; p53 is also required for apoptosis induced in response to DNA damage [45].

Table 20. Up-regulated proteins involved in apoptosis, CYT: cytoplasmic fraction; NE: nuclear fraction; fold change relative to controls in a logarithmic scale to the base 2; “-”, the protein was not detected in the respective samples.

Protein name	8h				24h			
	CYT		NE		CYT		NE	
	p value	fold change	p value	fold change	p value	fold change	p value	fold change
E3 ubiquitin-protein ligase TRIM33	-	-	-	-	1,24E-03	1,73	-	-
Peptidyl-tRNA hydrolase 2, mitochondrial	-	-	-	-	1,67E-02	1,35	-	-
Neutrophil gelatinase-associated lipocalin	-	-	-	-	4,47E-05	1,18	-	-
Programmed cell death protein 4	-	-	-	-	4,12E-02	0,99	-	-
Serine protease HTRA2, mitochondrial	2,99E-02	2,60	-	-	-	-	-	-
CDKN2A-interacting protein	2,57E-02	1,13	-	-	1,82E-02	-0,49	6,59E-04	0,66
Growth factor receptor-bound protein 2	-	-	1,45E-02	-2,03	1,87E-03	-0,53	7,26E-03	2,08

Serine/threonine-protein phosphatase 2A activator	-	-	-	-	-	-	1,19E-02	1,69
Merlin	-	-	-	-	-	-	2,16E-02	1,45
MRG-binding protein	-	-	1,28E-03	3,04	-	-	-	-
Death domain-associated protein 6	-	-	1,23E-04	2,93	-	-	-	-
Cyclin-L2	-	-	2,49E-02	1,19	-	-	1,27E-02	1,12
Mediator of DNA damage checkpoint protein 1	-	-	2,94E-02	1,10	-	-	2,98E-04	0,70
THO complex subunit 1	-	-	4,87E-02	1,33	-	-	-	-
CXXC-type zinc finger protein 5	-	-	-	-	-	-	4,51E-03	2,37

Increased ubiquitination and proteolysis was also observed (Table 21), suggesting that increased proteolytic degradation was occurring in response to the UCMG028 treatment. Protein E3 ubiquitin-protein ligase NEDD4, for example, is known to be involved in ubiquitination of growth factor receptor ErbB4, which builds a heterodimer with ErbB2 in the cell membrane. [46] Therefore, it is likely to think that proteolytic degradation of growth factor receptors was part of the mechanism of cell growth arrest induced by UCMG028.

Table 21. Up-regulation of proteins performing ubiquitination and peoteolysis, CYT: cytoplasmic fraction; NE: nuclear fraction; fold change relative to controls in a logarithmic scale to the base 2; “-“, the protein was not detected in the respective samples.

Protein name	8h				24h			
	CYT		NE		CYT		NE	
	p value	fold change	p value	fold change	p value	fold change	p value	fold change
Proteasome subunit beta type-10	-	-	1,69E-02	-1,35	3,15E-03	2,49	-	-

Proteasome subunit beta type-3	-	-	-	-	1,49E-02	1,11	2,20E-02	-3,46
E3 ubiquitin-protein ligase NEDD4	-	-	-	-	2,59E-03	0,95	-	-
Ubiquitin carboxyl-terminal hydrolase 48	8,87E-03	1,59	-	-	-	-	-	-
E3 ubiquitin-protein ligase UBR5	2,15E-02	1,82	-	-	-	-	3,06E-02	-0,69

Other up-regulated proteins found involved in cell growth arrest were also found to be up-regulated (Table 22). Among them one can find the insulin-like growth factor-binding protein 3, which is a part of the p53 signaling [47]. This protein is able to inhibit the growth promoting effect of Insulin-like growth factor receptors [48], which finally triggers apoptosis. [47]

Table 22. Up-regulation of proteins causing cell growth arrest, CYT: cytoplasmic fraction; NE: nuclear fraction; fold change relative to controls in a logarithmic scale to the base 2; “-“, the protein was not detected in the respective samples.

Protein name	8h				24h			
	CYT		NE		CYT		NE	
	p value	fold change	p value	fold change	p value	fold change	p value	fold change
Kunitz-type protease inhibitor 2	-	-	-	-	2,15E-02	1,63	-	-
Insulin-like growth factor-binding protein 3	-	-	-	-	1,52E-02	1,33	-	-
Prolyl 3-hydroxylase 1	-	-	-	-	4,86E-02	1,00	-	-
Ubiquitin carboxyl-terminal hydrolase BAP1	2,08E-02	1,12	-	-	-	-	-	-
MRG-binding protein	-	-	1,28E-03	3,04	-	-	-	-
Actin-like protein 6A	-	-	1,35E-02	1,44	-	-	-	-

Inhibitor of growth protein 5	–	–	2,67E-02	1,24	–	–	–	–
-------------------------------	---	---	----------	------	---	---	---	---

Finally, the observation that after 8 hours of incubation increased amounts of pyrroline-5-carboxylate reductase 1, which is involved in cellular response to oxidative stress, were detected, further supported the theory that the FASN inhibitor UCMG028 had actually induced oxidative stress in the SKOV3 cells.

Table 23. Up-regulation of a protein involved in response to oxidative stress, CYT: cytoplasmic fraction; NE: nuclear fraction; fold change relative to controls in a logarithmic scale to the base 2; “–”, the protein was not detected in the respective samples.

Protein name	8h				24h			
	CYT		NE		CYT		NE	
	p value	fold change	p value	fold change	p value	fold change	p value	fold change
Pyrroline-5-carboxylate reductase 1, mitochondrial	4,31E-03	1,09	–	–	–	–	–	–

3.3 Targeted metabolomics

3.3.1 Amino acids

All analyzed amino acids, except aspartic acid, glutamic acid and cysteine, gave sufficiently high signals and the estimated concentrations were within the quantification range. An exact quantitative analysis of every amino acid was possible with the help of calibration functions of the corresponding amino acids. Table 24 shows the estimated concentration differences of amino acids between control cells and with FASN inhibitor treated cells (8h and 24h). A negative value indicates amino acid down-regulation, while a positive value means amino acid up-regulation. Significant concentration differences are marked in green, while non-significant differences were marked in red.

Table 24. Estimated concentration differences of amino acids between control cells and with FASN inhibitor treated cells (8h and 24h). Results obtained from the FIA-MS/MS analysis.

Amino acid	Concentration difference 8h [μM]	Concentration difference 24h [μM]
Alanine	71,17	-144,17
Arginine	4,83	-37,17
Asparagine	22,33	-50,17
Glutamine	-605,00	-318,67
Glycine	-15,17	-80,65
Histidine	9,83	-24,87
Isoleucine	18,83	-54,35
Leucine	9,17	-55,17
Lysine	15,17	-11,80
Methionine	2,65	-12,38
Ornithine	0,30	-0,85
Phenylalanine	7,33	-26,93
Proline	13,17	-104,83
Serine	5,50	-15,18
Threonine	36,83	-53,17
Tryptophan	6,71	0,03
Tyrosine	16,33	-33,23
Valine	11,00	-43,50

Most significant concentration differences appeared after 24 hours of incubation and indicated down-regulation of many amino acids. There can be several explanations for the down-regulation of amino acids: in some cases a decreased amino acid uptake from the cell culture medium might have been occurred, since the neutral amino acid transporter (see section 3.3.1, Table 18) was also found to be down-regulated. Actually, amino acids transported by this proteine (glutamine, asparagine; aromatic amino acids such as tyrosine, phenylalanine; branched chain amino acids such as leucine, isoleucine, valine) were found to be down-regulated [49]. In case of histidine, the down-regulation can result from disruption of the β -alanine metabolism. In this process, carnosine is converted to histidine and β -alanine, β -alanine leading to the formation of acetyl-CoA and malonyl-CoA [50]. This hypothesis is supported by the accumulation (significant up-regulation) of carnosine (see section 3.3.2, Table 25).

3.3.2 Biogenic amines

Most quantitative values arising from the analysis of biogenic amines were valid (within the quantification range), with some exceptions of concentration values below the lower limit of quantification (LLOQ).

Table 25 shows all valid biogenic amines (concentration values within the quantification range) obtained from the FIA assay. A significant down-regulation of the biogenic amines cis-4-hydroxyproline and trans-4-hydroxyproline correlated with the down-regulation of proline from which they are synthesized. The same correlation was found for serotonin and kynurenine, which arise from tryptophan. [51]

Table 25. Concentration differences obtained from detected biogenic amines

Biogenic amine	Concentration difference 8h [μM]	Concentration difference 24h [μM]
Acetylornithine	-0,19	-0,50
alpha-Aminoadipic acid	-0,08	-0,62
cis-4-Hydroxyproline	-0,41	-4,68
Carnosine	0,43	0,37
Creatinine	-2,28	0,31
Kynurenine	-1,72	-4,98
Methioninesulfoxide	0,57	-0,13
Serotonin	0,12	-0,11
Spermidine	1,75	2,80
Spermine	-2,17	1,80
trans-4-Hydroxyproline	1,02	-4,10
Taurine	1,47	0,30

3.3.3 Phospholipids

In general, a disruption of the phospholipid biosynthesis was observed, as a vast majority of the glycerophospholipids and sphingolipids were down-regulated (see Tables 26 and 27). This effect of down-regulation became more pronounced after 24 hours, as significant differences arose from this incubation time. Besides the successful inhibition of FASN, an increased β -oxidation could also contribute to the concentration decrease of phospholipids. However, the results from the proteome profiling experiments controvert this hypothesis since proteins involved in β -oxidation have been found to be down-regulated (see section 3.2.2.1, Table 12).

Table 26. Concentration differences obtained from detected glycerophospholipids

Glucero-phospholipid	Concentration difference 8h [μM]	Concentration difference 24h [μM]
lysoPC a C14:0	0,72	-1,81
lysoPC a C16:0	-0,27	-5,02
lysoPC a C16:1	1,80	-4,78
lysoPC a C17:0	-0,05	-0,07
lysoPC a C18:0	-0,14	-0,92
lysoPC a C18:1	4,37	-7,08
lysoPC a C18:2	0,93	-0,05
lysoPC a C20:3	0,27	-0,58
lysoPC a C20:4	-0,44	-1,96
lysoPC a C24:0	-0,08	-0,57
lysoPC a C26:0	0,09	-0,87
lysoPC a C26:1	-0,04	-0,14
lysoPC a C28:0	-0,09	-0,39
lysoPC a C28:1	0,03	-0,10
PC aa C24:0	0,03	-0,35
PC aa C26:0	0,33	-1,58
PC aa C28:1	0,04	-0,51
PC aa C30:0	0,24	-5,35
PC aa C30:2	0,07	-0,10
PC aa C32:0	-6,82	-17,23
PC aa C32:1	-0,53	-18,52
PC aa C32:2	-1,03	-2,78
PC aa C32:3	-0,09	-0,19
PC aa C34:1	7,67	-56,00
PC aa C34:2	-2,38	-15,50
PC aa C34:3	-0,35	-1,61
PC aa C34:4	-0,05	-0,19
PC aa C36:0	-0,09	-0,66
PC aa C36:1	0,42	-7,07
PC aa C36:2	2,38	-18,27
PC aa C36:3	0,77	-3,88
PC aa C36:4	-0,74	-4,69
PC aa C36:5	-0,08	-0,93
PC aa C36:6	-0,03	-0,11
PC aa C38:0	-0,01	-0,81
PC aa C38:1	-0,01	-0,61
PC aa C38:3	-0,16	-2,78
PC aa C38:4	0,17	-2,30
PC aa C38:5	0,26	-3,20
PC aa C38:6	0,07	-1,68
PC aa C40:2	-0,01	-0,30
PC aa C40:3	-0,05	-0,40
PC aa C40:4	0,01	-0,42
PC aa C40:5	-0,07	-0,69
PC aa C40:6	0,28	-0,51
PC aa C42:0	-0,02	-0,06
PC aa C42:1	0,00	-0,10
PC aa C42:2	-0,02	-0,08

PC aa C42:4	-0,01	-0,06
PC aa C42:5	-0,01	-0,12
PC aa C42:6	-0,01	-0,16
PC ae C30:0	0,23	-1,72
PC ae C30:1	0,18	-0,53
PC ae C30:2	0,01	-0,10
PC ae C32:1	-0,17	-7,68
PC ae C32:2	0,10	-2,38
PC ae C34:0	-0,58	-1,38
PC ae C34:1	-0,40	-16,40
PC ae C34:2	0,50	-6,15
PC ae C34:3	0,00	-0,85
PC ae C36:0	-0,18	0,03
PC ae C36:1	0,07	-5,92
PC ae C36:2	0,79	-4,78
PC ae C36:3	0,62	-3,32
PC ae C36:4	-0,12	-4,55
PC ae C36:5	-0,16	-1,76
PC ae C38:0	0,06	-0,20
PC ae C38:1	-0,09	-1,85
PC ae C38:2	0,08	-2,38
PC ae C38:3	-0,06	-2,07
PC ae C38:4	0,05	-2,45
PC ae C38:5	-0,08	-3,78
PC ae C38:6	-0,15	-2,86
PC ae C40:1	0,00	-0,43
PC ae C40:2	-0,02	-0,73
PC ae C40:3	-0,02	-0,66
PC ae C40:4	-0,06	-0,78
PC ae C40:5	0,01	-1,16
PC ae C40:6	0,16	-1,17
PC ae C42:0	-0,04	-0,07
PC ae C42:1	0,02	-0,10
PC ae C42:2	-0,02	-0,11
PC ae C42:3	-0,07	-0,22
PC ae C42:4	-0,01	-0,21
PC ae C42:5	-0,01	-0,31
PC ae C44:3	-0,02	-0,09
PC ae C44:4	0,00	-0,05
PC ae C44:5	-0,01	-0,10
PC ae C44:6	0,01	-0,12

Table 27. Concentration differences obtained for sphingolipids

Sphingolipid	Concentration difference 8h [μM]	Concentration difference 24h [μM]
SM (OH) C14:1	0,06	-1,06
SM (OH) C16:1	-0,05	-0,80
SM (OH) C22:1	-0,05	-1,40
SM (OH) C22:2	0,16	-1,60
SM (OH) C24:1	0,04	-0,43
SM C16:0	1,82	-30,07
SM C16:1	0,13	-2,34
SM C18:0	0,09	-3,85
SM C18:1	0,18	-1,24
SM C20:2	0,01	-0,03
SM C24:0	0,30	-4,88
SM C24:1	0,67	-11,34
SM C26:0	-0,01	-0,07
SM C26:1	-0,03	-0,22

3.3.4 Acylcarnitines

Acylcarnitines are the transport form of fatty acids through the mitochondrial membrane into the mitochondrial matrix, where they are introduced into the β -oxidation pathway. [6] As shown in Table 28, lower amounts of acylcarnitines after treatment with UCMG028 were detected. Since acylcarnitines arise from glycerophospholipids, a decrease of the glycerophospholipid concentration in treated SKOV3 cells inevitably leads to lower acylcarnitine levels as well. The lower amount of this metabolite class is another evidence for impaired energy supply as a result of the blockade of fatty acid biosynthesis.

Table 28. Concentration differences obtained from detected acylcarnitines

Acylcarnitine	Concentration difference 8h [μM]	Concentration difference 24h [μM]
C0	0,55	1,01
C10	0,01	-0,11
C10:1	-0,01	-0,05
C10:2	0,01	-0,03
C12	0,00	-0,02
C12-DC	0,00	-0,01
C12:1	0,00	-0,04
C14	0,01	-0,01
C14:1	0,01	-0,05
C14:1-OH	0,00	-0,01
C14:2	0,00	-0,01
C14:2-OH	0,01	-0,04
C16	-0,01	-0,02
C16-OH	0,01	-0,01
C16:1	0,01	-0,03
C16:1-OH	0,01	-0,08
C16:2	0,00	-0,01
C16:2-OH	0,01	-0,03
C18	0,01	-0,01
C18:1	0,01	-0,04
C18:1-OH	0,01	-0,02
C18:2	0,00	-0,02
C2	0,01	1,83
C3	0,00	0,05
C3-OH	0,01	-0,10
C3:1	0,01	-0,09
C4	-0,04	-0,14
C3-DC (C4-OH)	0,02	-0,15
C4:1	0,01	-0,05
C5	0,02	0,04
C5-M-DC	0,04	-0,39
C5-OH (C3-DC-M)	0,08	-0,78
C5:1	0,01	-0,04
C5:1-DC	0,01	-0,08
C6 (C4:1-DC)	0,00	-0,03
C5-DC (C6-OH)	0,01	-0,08
C6:1	0,01	-0,03
C7-DC	0,00	-0,01
C8	0,00	0,12
C9	0,01	-0,03

3.3.5 Hexose

A decrease of the hexose levels was also observed; a significant down-regulation appeared after 24 hours of incubation (Table 29). An explanation for this effect can be that the cells produce more of their energy through the glycolytic pathway, which may be a way for the cells to ensure their energy production as alternative to the β -oxidation which was down-regulated.

Table 29. Concentration differences of hexose from both methods FIA-MS/MS and LC-MS/MS

Analyte	Concentration difference 8h [μ M]	Concentration difference 24h [μ M]
Hexose	-60	-224

4 Discussion

The objective of this master thesis was to assess the effects of the fatty acid synthase inhibitor UCMG028 on the ovarian cancer cell line SKOV3 which is known to overexpress FASN [5]. UCMG028 was designed with the intention to overcome the limitations of existing FASN blockers. Expected effects caused by FASN inhibition, which have made the fatty acid synthase a promising target for anticancer therapy, are cell cycle- and cell growth arrest and induction of apoptosis. All these effects were indeed observed after treatment of cells with UCMG028.

Evidence for the inhibition of FASN after incubation with UCMG028 was provided from proteome profiling and targeted metabolomics experiments. A gradual decrease of the phospholipid concentration in the course of incubation with this drug was observed, however, a significant down-regulation of FASN metabolites did not appear before 24h of incubation. The overall decrease of glycerophospholipids observed from the targeted metabolomics assay may be a consequence of two different events: increased phospholipid consumption for β -oxidation or decreased synthesis of palmitic acid, which is the precursor of all fatty acids needed for biosynthesis of all lipids (e.g. glycerophospholipids, sphingolipids). The first hypothesis can be rejected since several proteins involved in β -oxidation proved to be down-regulated, suggesting a decrease of energy supply via β -oxidation. In addition, significant decrease of the glucose level, observed after 24h of incubation, may imply that the alternative glycolytic pathway for energy production have been stimulated in the cells as a response to impaired β -oxidation. Moreover, sphingolipids, which are not involved in β -oxidation, were found to be down-regulated as well. Concentration decline of such a variety of lipids in the ovarian cancer cells implies down-regulation of the synthesis of their mutual precursor, which is palmitic acid.

As a consequence of the reduced phospholipid supply, cell growth is also affected, as glycerophospho- and sphingolipids contribute to the formation of lipid rafts. These microstructures accommodate growth factor receptors, transporters and other proteins with a glycosylphosphatidylinositol-lipid anchor. [52] Interference with proper membrane formation can result in degradation of membrane proteins such as the above mentioned growth factor receptors or transporters. Actually, this may account for the observed down-regulation of neutral amino acid transporters. Furthermore, inhibition of the biosynthesis of palmitic acid also leads to accumulation of its precursors such as malonyl-CoA. In turn, high malonyl-CoA levels in the cell lead to the inhibition of the synthesis of further malonyl-CoA, resulting from a negative feedback mechanism. [6] This would explain the down-regulation of acetyl-CoA carboxylase, which catalyses the formation of malonyl-CoA, observed in the UCMG028 treated cells. Inhibition of FASN activity also leads to accumulation of NADPH and formation of reactive oxygen species (ROS) (see Figure 5). The down-regulation of superoxide dismutase [Cu-Zn], whose task is to destroy free radicals in

the cell, contributes to the increased ROS concentrations. This would explain why proteins involved in the cellular response to oxidative stress were up-regulated as well. This accounts for pyrroline-5-carboxylate reductase 1, which was found to be up-regulated after 8h of incubation. Thus, as previously reported, inhibition of the fatty acid synthesis not only caused cytostatic but also cytotoxic effects in ovarian cancer cells.

As mentioned previously, inhibition of FASN is accompanied by cytostatic effects on ovarian cancer cells. Considering the data from the proteome profiling experiments, one can conclude that treatment with UCMG028 shows the expected cytostatic effect. Down-regulation of proteins involved in mitotic processes (formation of the mitotic spindle apparatus, chromosome segregation, cytokinesis, and transition from one mitotic phase to another) gave a hint that cell cycle disruption has taken place. This assumption is supported by the simultaneous raise of several proteins participating in the inhibition of cell division such as proteins disrupting the tubulin assembly and proteins repressing transcriptional activity required for cell cycle progression. The cytostatic effect of the FASN inhibitor was further apparent from the observation that proteins involved in cell growth arrest were also affected. Indeed, EGFR- and mTOR signaling as well as estrogen induced cell growth signaling were down-regulated. Down-regulation of proteins may occur via ubiquitination followed by protein degradation. This mechanism could also have occurred in the SKOV3 cells as several proteins performing degradation and proteolysis were found to be up-regulated, while mTOR levels decreased. Among these degrading proteins, there was NEDD4. Actually, this protein ubiquitinates growth factor receptor ErbB4; ErbB4 builds a heterodimer with ErbB2 in the cell membrane. Thus, the observed cell growth arrest may have occurred according to the events illustrated in Figure 5, showing that attenuation of the synthesis of lipids necessary to form membrane lipid rafts leads to the degradation of cell growth factor receptors usually accommodated in these cell membrane compartments, which results in inhibition of cell growth.

While the cell cycle progression in the SKOV3 cell line was blocked, apoptotic pathways were activated. As already mentioned, Uddin *et al.* discovered a disruption of the mitochondrial membrane integrity after treatment of epithelial ovarian carcinoma (EOC) with the FASN blocker C75, followed by induction of apoptosis via the mitochondrial pathway [7]. Down-regulation of mitochondrial membrane proteins can also give a hint that the stability of mitochondria in SKOV3 was affected, resulting in release of cytochrome c into the cytosol, followed by apoptosis. Several proteomic analyses identified a large amount of mitochondrial proteins in lipid rafts, including ATP synthase, prohibitin, VDAC1 and 2, isocitrate dehydrogenase and calreticulin. Based on these findings, the existence of raft-like domains in mitochondria cannot be excluded. [53] This suggests that a decreased supply of phospholipids due to down-regulation of their biosynthesis could also disturb the mitochondrial membrane stability with subsequent degradation of the mitochondrial membrane proteins. Another explanation for the down-regulation of mitochondrial membrane proteins observed after FASN inhibition may also be considered. Based on our results, it can

be assumed that severe DNA damage has taken place as a result of oxidative stress induced in the cells, followed by activation of the p53 signaling and apoptosis via the mitochondrial pathway. Early apoptotic stages after 8h of incubation seem probable, as an increase of the amount of the THO complex subunit 1, which activates caspase-6, was observed. Later stages of apoptosis going along with activation of caspase-3 could not be detected, which might be due to insufficient incubation time.

In parallel with the induction of the apoptotic pathway, several oncogenic pathways important for cell survival, such as the MAPK, the Ras and the NFκB signaling pathway, seemed to be impaired. Down-regulation of MAPK signaling, indicated by degradation of the proteins belonging to this pathway, has already been demonstrated by Grunt *et al.* [5]. However, attenuation of the Ras and NFκB cascades caused by FASN inhibition has not been described yet. The commonly accepted view is that activation of the NFκB signaling leads to resistance to apoptosis, [54] for example by activating the inhibitor of apoptosis proteins (IAPs). [55] Therefore, down-regulation of signaling cascades involved in cell survival, such as the NFκB signaling, can be a result of induced apoptosis. The role of the Ras signaling pathway is to mediate signal transduction from plasma membrane receptors to the nucleus. [56] It has been shown that this pathway protects cells from apoptosis either through activation of PKB/Akt via PI3-kinase or through activation of NFκB. [57] Downregulation of the PI3K cascade induced by blockade of the FASN activity has already been reported. [5]

Acylcarnitines levels also showed a significant reduction after 24h of drug treatment. These compounds are formed from the reaction of carnitine and fatty acids. Thus, one can expect that reduction of fatty acid synthesis will also cause reduction of acylcarnitines. Another reason for the lower acylcarnitine concentrations can be an impaired function or degradation of the carnitine-acylcarnitine translocase. This mitochondrial membrane protein transports carnitine from the mitochondrial matrix to the cytosol, where acylcarnitines are synthesized. [6] Thus, if the above mentioned hypothesis that the mitochondrial membrane integrity was affected upon incubation with the FASN blocker is true, one can assume that the function of the transporter protein has also been disrupted and/or its degradation has occurred.

It is clear that impaired formation of membrane lipid rafts causes severe disruption of important cell signaling and intracellular transport. This may also be reflected in decreased amino acid uptake in the ovarian cancer cells as a result of the lack of membrane transporters accommodated in these lipid-protein microdomains. It is known that membrane transporters are accommodated in membrane lipid rafts. [45] If amino acid transporters are among these proteins, one can assume that, such as in case of ErbB2, abrogated lipid raft formation also negatively affects membrane localization of amino acid transporters in the cell membrane, leading to their degradation. This hypothesis may explain the down-regulation of the neutral amino acid transporter B(0), followed by decreased concentrations of the corresponding neutral amino acids in the cells. The decreased amino acid uptake apparently had

also consequences on the biosynthesis of proteins and those are essential for the performance of cellular functions and other metabolic processes. Actually, a decreased uptake of tryptophan and thus an attenuated tryptophan metabolism manifested itself in a decrease of the corresponding tryptophan metabolites serotonin and kynurenine. This has a negative impact on energy metabolism, since kynurenine is used for the production of nicotinic acid [58], whose derivatives are NADH, NAD, NAD⁺ [59]. Pyruvate synthesis was also affected, caused by decreased levels of amino acids such as tryptophan (through the nicotinamide metabolism), [60] alanine [61] and proline. [62] Pyruvate plays a central role in the metabolism of carbohydrates, proteins and fats. [63] The reasons why other metabolic processes were also affected have to be clarified yet, for example, the down-regulation of cysteine biosynthesis, the impaired formation of tyrosine from tryptophan, and the accumulation of carnosine used for synthesis of histidin. It may, however, be considered that they will have an impact on the production of pyruvate (from cysteine) [6] and on the CoA biosynthesis (from carnosine via the β -alanine metabolism). [64]

5 Conclusion

Based on the presented results, one can conclude that the FASN inhibitor UCMG028 is a promising anticancer agent for treatment of epithelial ovarian malignancies. Blockade of the fatty acid synthase activity by this drug induced abrogation of cellular processes essential for tumor growth and progression such as cell growth and proliferation. It was also demonstrated that the cell viability of the ovarian cancer cell line SKOV3 is affected by this drug due to cytotoxic effects triggering programmed cell death. In conclusion, the FASN inhibitor UCMG028 does not only have the potential of inhibiting tumor growth, but also of decreasing the tumor size. Considering the results from the proteome profiling experiments, which showed that only a small number of pathways apart from those already known to be related to FASN inhibition were affected, it is likely that this drug selectively inhibits FASN. The selective inhibition of FASN with a minimal amount of side reactions is essential for the selectivity of the therapeutic agent against ovarian carcinomas and hence for its future clinical application.

References

- [1] Veigel, D.; Wagner, R.; Stübiger, G.; Wuczkowski, M.; Filipits, M.; Horvat, R.; Benham, B.; López-Rodríguez, M. L.; Leisser, A.; Valent, P.; Grusch, M.; Hegardt, F. G.; García, J.; Serra, D.; Auersperg, N.; Colomer, R.; Grunt, T. W.; Fatty acid synthase is a metabolic marker of cell proliferation rather than malignancy in ovarian cancer and its precursor cells *Int. J. Cancer*: 00, 00–00 (2014)
- [2] Jiang, L.; Wang, H.; Li, J.; Fang, X.; Pan, H.; Yuan, X.; Zhang, P.; Up-Regulated FASN Expression Promotes Transcoelomic Metastasis of Ovarian Cancer Cell through Epithelial-Mesenchymal Transition *Int. J. Mol. Sci.* 2014, 15: 11539-11554
- [3] Anderson, A.S.; Roberts, P.C.; Frisard, M.I.; McMillan, R.P.; Brown, T.J.; Lawless, M.H.; Hulver, M.W.; Schmelz, E.M.; Metabolic Changes During Ovarian Cancer Progression as Targets for Sphingosine Treatment *Exp Cell Res.* 2013 June 10; 319(10): 1431–1442
- [4] Flavin, R.; Peluso, S.; Nguyen, P. L.; Loda M.; Fatty acid synthase as a potential therapeutic target in cancer *Future Oncol.* **2010** April ; 6(4): 551–562
- [5] Tomek, Ch.; Wagner, Varga, F.; Singer, Ch. F.; Karlic, H.; Grunt, T. W.; Blockade of Fatty Acid Synthase Induces Ubiquitination and Degradation of Phosphoinositide-3-Kinase Signaling Proteins in Ovarian Cancer *Mol Cancer Res* 2011;9:1767-1779
- [6] Berg, J. M.; Tymoczko J. L.; Stryer L.; Biochemie 2007, 6. Auflage
- [7] Uddin, S.; Jehan, Z.; Ahmed, M.; Alyan, A.; Al-Dayel, F.; Hussain, A.; Bavi, P.; Al-Kuraya, K. S.; Overexpression of Fatty Acid Synthase in Middle Eastern Epithelial Ovarian Carcinoma Activates AKT and Its Inhibition Potentiates Cisplatin-Induced Apoptosis **2011** *Mol. Med.* 17 (7-8) 635-645
- [8] Paraiso, K. H. T.; Van Der Kooi, K.; Messina, J. L.; Smalley, K. S. M.; Measurement of constitutive MAPK and PI3K/AKT signaling activity in human cancer cell lines *Methods Enzymol. Author manuscript; available in PMC* 2014 Apr 28.
- [9] Grunt, T. W.; Wagner, R.; Grusch, M.; Berger, W.; Singer, Ch. F.; Marian, B.; Zielinski, Ch. C.; Lupu, R.; Interaction between fatty acid synthase- and ErbB-sysyems in ovarian cancer cells *Biochemical and Biophysical Research Communications* 385 (2009) 454-459
- [10] Menendez, J.A.; Lupu, R.; Fatty acid synthase and the lypogenic phenotype in cancer pathogenesis) *Nature Reviews Cancer* **7**, 763-777 (October 2007)

[11] Koromilas, A.; Tenkerian, C; Krishnamoorthy, J.; Kamindla, R.; Wang, S.; Control of cell fate by the mammalian target of rapamycin (mTOR) under stress depends on eIF2 α serine 51 phosphorylation. *Ann. Oncol.* 2015

[12] <http://www.uniprot.org/uniprot/P31749>

[13] Moore, R.G.; Lange, Th.S.; Robinson, K.; Kim, K.K.; Uzun, A.; Horan, T.C.; Kavar, N.; Yano, N.; Chu, S.R.; Mao, Q.; Brard, L.; DePaepe, M.E.; Padbury, J. F.; Arnold, L.A.; Brodsky, A.; Shen, T-L.; Singh, R.K.; Efficacy of a Non-Hypercalcemic Vitamin-D2 Derived Anti-Cancer Agent (MT19c) and Inhibition of Fatty Acid Synthesis in an Ovarian Cancer Xenograft Model; *PloS ONE*, April 2012/Vol. 7/Issue 4 e34443

[14] Anderson, N. L.; Anderson N. G. Proteome and proteomics: New technologies, new concepts, and new words *Electrophoresis* **1998**, 19, 1853-1861

[15] Dhingra, V.; Gupta, M.; Andacht, T.; Fu, Z. F.; New frontiers in proteomics research: A perspective **2005** *Internal Journal of Pharmaceutics*, Vol. 299, pages 1-18

[16] McDonald, H.W.; Yates, J.R.; Shotgun proteomics and biomarker discovery; *Disease Markers* 18 (2002) 99–105

[17] Integrative proteomics by Dr. Hon-Chiu Leung (Ed.) 2012

[18] Proteomics Sample Preparation by Jörg von Haagen (Ed.) 2008

[18] Lottspeich, F.; Engels, J. W.; Bioanalytik 3. Auflage 2012

[20] <http://blast.ncbi.nlm.nih.gov/Blast.cgi>

[21] https://www.biochem.mpg.de/221765/Mass_spectrometry

[22] Scheltema, R. A.; Hauschild J-P.; Lange O.; Hornburg D.; Denisov E.; Damoc E.; Kuehn A.; Makarov A.; Mann M. The Q Exactive HF, a Benchtop Mass Spectrometer with a Pre-filter, High Performance Quadrupole and an Ultra-High Field Orbitrap Analyzer *MCP Papers in Press. Published on October 30, 2014 as Manuscript M114.043489*

[23] <http://planetorbitrap.com/q-exactive#tab:schematic>

[24] Makarov A. A. U.S. Patent 5,886,346, 1999

[25] Dienes, T.; Pastor, S. J.; Schurch, S.; Scott, J. R.; Yao, J.; Cui, S.; Wilkins, C.L. *Mass Spectrom. Rev.* **1996**, 15, 163-211

[26] Hao, Z.; Zhang, Y.; Shannon Eliuk , Blethrow, J.; Horn, D.; Zabrouskov, V.; Kellmann, M.; Huhmer, A. F.; A Quadrupole-Orbitrap Hybrid Mass Spectrometer

Offers Highest Benchtop Performance for In-Depth Analysis of Complex Proteomes
©2012 Thermo Fisher Scientific Inc.

[27] Cox, J.; Mann, M.; MaxQuant enables high peptide identification rates, individualized p.p.b.-range mass accuracies and proteome-wide protein quantification
2008 *Nature biotechnology*

[28] http://www.matrixscience.com/search_intro.html

[29] Powers, R.; The Current State of Drug Discovery and a Potential Role for NMR Metabolomics *J. Med. Chem.* 2014, 57, 5860-5870

[30] Zhou, B.; Xiao, J. F.; Tuli, L.; Ransom, H. W.; LC-MS-based metabolomics *Mol. Biosyst.* 2012 Feb; 8(2): 470-481

[31] Chung, K.A.; Fan, H.; Hyphenation of Flow-Injection Analysis with Mass Spectrometry: A Versatile and High-Throughput Technique *Spectroscopy* 2012

[32] Boja, E. S.; Rodriguez, H.; The Path to Clinical Proteomics Research: Integration of Proteomics, Genomics, Clinical Laboratory and Regulatory Science *Korean J Lab Med* 2011 Apr; 31(2): 61-71

[33] Biocrates Absolute/IDQ™ p180 Kit user manual

[34] Laplante, M.; Sabatini, D.M.; mTOR signaling in growth control and disease *PMC Apr.* 2013

[35] http://www.genome.jp/dbget-bin/www_bget?map04010

[36] http://www.genome.jp/dbget-bin/www_bget?map04014

[37] <http://www.uniprot.org/uniprot/Q16512>

[38] <http://www.uniprot.org/uniprot/Q9Y6X8>

[39] <http://www.uniprot.org/uniprot/P30307>

[40] <http://www.uniprot.org/uniprot/P47736>

[41] <http://www.uniprot.org/uniprot/Q96FV9>

[42] http://www.kegg.jp/dbget-bin/www_bget?ec:3.4.22.59

[43] <http://www.uniprot.org/uniprot/Q13489>

[44] http://www.genome.jp/kegg-bin/show_pathway?ko04210

[45] Alberts, B.; Johnson, A.; Lewis, J.; Raff, M.; Roberts, K.; Walter, P.; Molecular Biology of the Cell. 4th edition. 2002

[46] <http://www.uniprot.org/uniprot/P46934>

- [47] http://www.kegg.jp/kegg-bin/show_pathway?ko04115+K10138
- [48] <http://www.uniprot.org/uniprot/P17936>
- [49] <http://www.uniprot.org/uniprot/Q15758>
- [50] http://www.kegg.jp/kegg-bin/show_pathway?map00410+C00386
- [51] http://www.kegg.jp/kegg-bin/show_pathway?map00380+C00780
- [52] Merrill, A. H.; Sandhoff, K.; Biochemistry of Lipids, Lipoproteins and Membranes 4th edition, 2002 Elsevier Science B.V.
- [53] Pike, L. J.; The challenge of lipid rafts *J Lipid Res.* 2009 Apr; 50(Suppl): S323–S328.
- [54] Meteoglu, I.; Erdogdu, I.H.; Meydan N.; Erkus, E.; Barutsa, S.; NF-KappaB expression correlates with apoptosis and angiogenesis in clear cell renal cell carcinoma tissues *Journal of Experimental & Clinical Cancer Research* 2008, **27**:53
- [55] http://www.genome.jp/kegg-bin/show_pathway?map04210
- [56] Radziwill, G.; Erdmann, R.A.; Margelish, U.; Moelling, K.; The Bcr Kinase down-regulates Ras signaling by phosphorylating AF-6 and binding to its PDZ domain *Mol Cell Biol.* 2003 Jul; 23(13): 4663–4672.
- [57] Downward, J.; Ras signaling and apoptosis *Curr Opin Genet Dev.* 1998 Feb;8(1):49-54
- [58] <http://www.hmdb.ca/metabolites/HMDB00684>
- [59] <http://www.hmdb.ca/metabolites/HMDB01488>
- [60] http://www.genome.jp/kegg-bin/show_pathway?map00760
- [61] http://www.genome.jp/kegg-bin/show_pathway?map00250
- [62] http://www.genome.jp/keggbin/show_pathway?scale=1.0&query=pyruvate&map=map00330&scale=&auto_image=&show_description=hide&multi_query=
- [63] <http://www.hmdb.ca/metabolites/HMDB00243>
- [64] http://www.kegg.jp/kegg-bin/show_pathway?map00410+C00386

Appendix

1. Materials

1.1 Cell culture experiments

- Thermo Fisher Scientific Herasafe KS laminar flow cabinet
- Thermo Fisher Scientific Heracell 150i CO₂ incubator
- Thermo Fisher Scientific Megafuge 16R centrifuge
- Falcon™ Cell Culture Flask (25cm²: 353109; 75cm²: 353024)
- ZEISS Primo Vert microscope
- Sterile pipettes
- Falcon™ Polypropylene Conical Tubes 15ml
- Bandelin Sonopuls UW 2070 homogeniser
- Moxi™ Mini automated cell counter by Orflo
- Julabo ED Heating Emersion Circulator
- Multwell™ 6 Well plates

1.2 Cell disruption

- Ice
- Terumo Syringe 5ml (SSO5SE1)
- Terumo Neolus 23G needles (NN2332R)
- desiccator/aspirator (pump)
- Corning Incorporated costar® Cell Scraper
- Thermo Fisher Scientific Megafuge 16R centrifuge
- Bandelin Sonorex Digital 10P Ultrasonic bath
- Eppendorf Safe-Lock Tubes 1.5ml

1.3 1D SDS-PAGE

- Mini-Protean™-Cell Tetra System electrophoresis unit by BIO-RAD (1mm spacer)
- desiccator/aspirator (pump)

- filtering paper
- Kaiser prolite basic 2 light box
- GFL 3016 laboratory shaker

1.4 Shotgun proteomics

- Eppendorf Centrifuge 5424
- Nanosep[®] Centrifugal Device with Omega membrane MWCO 3kDa
- Pierce C-18 Spin Columns by Thermo Scientific
- Thermo Scientific Heratherm incubator by PALL Life Sciences
- Sigma-Aldrich Clear-view[®] Snap-Cap microtubes, Size 0.6ml, siliconized
- Eppendorf Thermomixer[®] Comfort
- miVac Duo concentrator by GeneVac
- Dionex Ultimate 3000 RSLC nano System
- Thermo Fischer Scientific Q Exactive mass spectrometer
- Eppendorf Safe-Lock Tubes 1.5ml

1.5 Targeted metabolomics

- Absolute/*IDQ*[®] p180 Kit by Biocrates Life Sciences
- Thermo Fisher Scientific Megafuge 16R centrifuge
- IKA[®] WORKS Vortexer

2 Reagents

2.1 Cell culture

- Sigma Penicillin-Streptomycin with 10 000 units penicillin and 10 mg streptomycin per ml in 0,9% NaCl, P0781
- Gibco[®] GlutaMAX[™] MEM α cell culture medium
- Fetal Bovine Serum, Research grade by SIGMA-ALDRICH[®], F0804-50ml
- L-Glutamine (200mM) by Gibco[®]
- 0.1% DMSO solution
- UCMG028 (20mg/ml) in 0.1% DMSO

2.2 Harvesting of cells

2.2.1 Proteome profiling

- Phosphate buffer (PBS) (Table 1)
- Ethanol
- Sample buffer (see Table 2)
- Urea
- Isotonic cell lysis buffer (see Table 3)
- Proteasom inhibitor cocktail (PIC) (see Table 4)
- 100mM Phenylmethylsulfonylfluorid (PMSF) (see Table 5)
- TE_{NaCl} (see Table 6)
- TE_{NP40} (see Table 7)

2.2.2 Targeted metabolomics

- Ethanol/Phosphate buffer (10mM NaH₂PO₄/Na₂HPO₄ pH=7.5) (85/15)

2.3 1D-SDS-PAGE

- Stock solutions for separating gel and stacking gel
- Separating gel (see Table 8)
- Stacking gel (see Table 9)
- Molecular weight marker: Precision Plus Protein™ Standards-Dual Color by BIO-RAD (161-0374)
- 5x SDS buffer (see Table 23)
- Electrode buffer (see Table 11)

2.4 Silver staining

- 50% methanol / 10% acetic acid (see Table 12)
- 50% methanol (see Table 13)
- 0.02% sodium thiosulfate (see Table 14)
- 0.1% AgNO₃ (see Table 15)
- 3% Na₂CO₃/0.05% HCHO (see Table 16)
- 1% acetic acid

2.5 Protein digestion

- 500mM ABC buffer (see Table 17)
- 50mM ABC buffer
- 25mM ABC buffer
- 1M DTT stock solution (for in-solution digestion) (see Table 20)
- 500mM IAA stock solution (for in-solution digestion) (see Table 21)
- Trypsin sequencing grade, modified by Promega #V5111
- ACN/water 1:1
- 5% ACN/ 0.5% TFA solution
- 10% TFA solution
- 50% ACN/ 0.1% TFA solution
- DTT reagent (for in-solution digestion): 5mg/ml DTT, 8M GHCl
- IAA reagent (for in-solution digestion): 10mg/ml DTT, 8M GHCl
- 5% Formic acid

2. Production of solvents and reagents

Table 1. PBS buffer

(phosphate buffered saline, pH 7.3; storage: 4°C) Volume = 10l

NaCl	80g
KCl	2g
KH ₂ PO ₄	2g
Na ₂ HPO ₄ x 2H ₂ O	14.4g
Dest. H ₂ O	10l

Table 2. Sample Buffer

(storage: 1ml aliquotes at -20°C) Volume = 50ml

7.5M Urea	22.5g Urea
1.5M Thiourea	5.7g Thiourea
4% CHAPS	2g CHAPS
0.05% SDS	125µl 20% SDS
100mM DTT	5ml 1M DTT
Dest. H ₂ O	50ml

Table 3. Isotonic lysis buffer

(storage: 4°C, Volume: 100ml)

10mM HEPES/NaOH pH 7.4	1ml 1M HEPES/NaOH pH 7,4
10mM NaCl	200µl 5M NaCl
0.5mM MgCl ₂	50µl 1M MgCl ₂
1mM EGTA	500µl 0.2M EGTA
0.25M Sucrose-Lösung	2.5ml 2M sucrose solution
0.5% Triton X-100	500µl 20% Triton X-100
dest. H ₂ O	100ml

Table 4. PIC (freshly prepared)

Dest H ₂ O	880µl
Pepstatin A [1mg/ml in ethanol]	100µl
Leupeptin [10mg/ml in H ₂ O]	10µl
Aprotinin [10mg/ml in 0.01M HEPES/NaOH pH 8.0]	10µl

Table 5. PMSF (storage: 4°C) Volume = 100ml

Phenylmethylsulfonylfluorid	1.742g
Propanol-2	100ml

Table 6. TE_{NaCl} (storage 4°C, Volume = 100ml)

10mM Tris/HCl pH 7.4	1ml 1M Tris/HCl pH 7.4
1mM EDTA pH 7.5	200µl 0.5M EDTA pH 7.5
500mM NaCl	10ml 5M NaCl
dest. H ₂ O	100ml

Table 7. TE_{NP40} (storage: 4°C, Volume = 100ml)

10mM Tris/HCl pH 7.4	1ml 1M Tris/HCl pH 7.4
1mM EDTA pH 7.5	200µl 0.5M EDTA pH 7.5
10% NP40	5ml
dest. H ₂ O	100ml

Table 8. Separating gel (freshly prepared)

12% acryl amide	2.4ml 30% AA/PDA
375mM Tris-HCl pH 8.8	1.125ml 2M Tris-HCl pH 8.8

dest. H ₂ O	2.415ml
For polymerization:	
0.1% SDS	50µl 20% SDS
0.045% APS	45µl 10% APS
0.075% TEMED	3.8µl TEMED

Table 9. Stacking gel (freshly prepared)

4% acryl amide	0.533ml 30% AA/PDA
125mM Tris-HCl pH 6.8	0.5ml 2M Tris-HCl pH 6.8
dest. H ₂ O	2.93ml
For polymerization:	
0.1% SDS	20µl 20% SDS
0.045% APS	20µl 10% APS
0.075% TEMED	4µl TEMED

Table 10. Corck gel (freshly prepared)

Separating gel (without polymerization reagents)	1ml
0.045% APS	10µl
0.075% TEMED	2.5µl

Table 11. Electrode buffer (stored at room temperature, Volume = 1l)

dest. H ₂ O	895ml
25mM Tris/192mM Glycine	100ml 10x Tris/Glycine (30g/144g/1l)
0.1% SDS	5ml 20% SDS (20g/100g)

Table 12. Fixing solution (stored at room temperature, Volume = 5l)

50% methanol	2500ml 100% methanol
10% acetic acid	500ml 100% acetic acid
H ₂ O	2000ml

Table 13. 50% Methanol solution (stored at room temperature, Volume = 1l)

50% methanol	500ml 100% methanol
50% water	500ml bidest. water

Table 14. Sensitising solution (freshly prepared, 50ml)

0.02% sodium thiosulfate	0.5ml 2% $\text{Na}_2\text{S}_2\text{O}_3 \cdot 5\text{H}_2\text{O}$
bidest. water	49.5ml

Table 15. Silver impregnation solution (freshly prepared, 50ml)

0.1% AgNO_3	0.5ml 10mg/ml AgNO_3 stock solution (4°C)
bidest. water	49.5ml

Table 16. Developing solution (freshly prepared, 50ml)

Na_2CO_3	1.5g
bidest. water	50ml
37% HCHO	65µl HCHO

Table 17. 500mM ABC buffer (freshly prepared, stored for no more than 2 days at 4°C)

$(\text{NH}_4)\text{HCO}_3$	0.2g
dest. water	5ml

Table 18. Trypsin stock solution (stored in 10µl aliquots at -80°C)

Trypsin/LysC mix	20µg
50mM acetic acid	200µl

Table 19. Destaining solution (freshly prepared, 10ml)

15mM $K_3Fe(CN)_6$	1ml 150mM $K_3Fe(CN)_6$ (0.4938g/10ml H_2O , stored at 4°C)
50mM $Na_2S_2O_3$	1ml 500mM $Na_2S_2O_3$ (1.2409g/10ml H_2O , stored at 4°C)
dest. water	8 ml

Table 20. 1M DTT stock solution (for in-gel digestion, stored in 900µl aliquots at -20°C)

DTT	1.5425g
50mM ABC buffer	10ml

Table 21. 500mM IAA stock solution (for in-gel digestion, stored in 900µl aliquots at -20°C)

IAA	0.9248g
50mM ABC buffer	10ml

Table 22. Phosphate buffer (pH 7.4, stored st 4°C, Volume = 200ml)

10mM NaH_2PO_4	0.452ml 1M NaH_2PO_4 (0.2764g $NaH_2PO_4 \cdot xH_2O$ in 2ml H_2O)
10mM Na_2HPO_4	1.548ml 1M Na_2HPO_4 (0.3559g $Na_2HPO_4 \cdot x2H_2O$ in 2ml H_2O)
dest. water	200ml

Table 23. 5xSDS buffer (storage 4°C, 20ml)

250mM Tris.Cl pH 6.8	5ml 1M Tris.Cl pH 6,8
10% SDS	2g SDS
50% Glycerol	10ml Glycerol
0.25% Bromophenol-Blue	0.05g Bromophenol-Blue
A.dest	17,5ml

Mix before use: 437.5µl 5xSDS buffer+ 62.5µl 2- mercaptoethanol

Curriculum vitae

Name: Mariya Evgenieva Semkova

Date of Birth: January 22nd, 1990

Education:

2013-2015: University of Vienna, Faculty of Chemistry, Master Degree in
Chemistry

2009-2013: University of Vienna, Faculty of Chemistry, Bachelor Degree in
Chemistry

2009: Graduation at the European School Mol, Belgium